Detection of neutral particles

detection of neutrons

detection of neutrinons

detection of low energy photons

(detection of high energy photons → calorimeters)

Detection of neutral particles

Detection of neutral particles = let them interact with the detector medium, detect resulting charged particles.

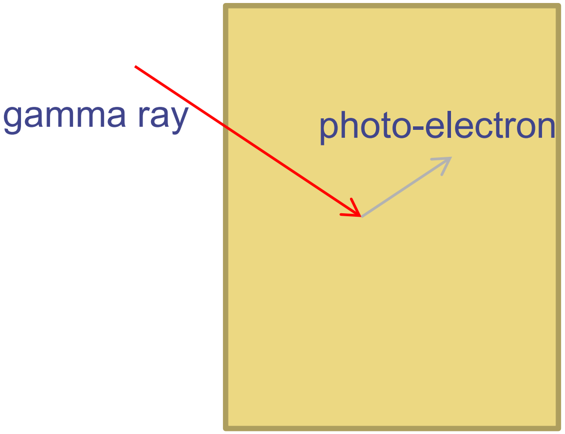

Interaction of low energy photons with matter - 1

Photoeffect:

- $E^{-3.5} Z^5$ + discontinuities (around electron binding energies)
- all energy absorbed

Compton effect:

- Z lnE/E
- only part of photon energy transferred to the electron

Pair production: Z^2, important much above the threshold ($2m_e$)

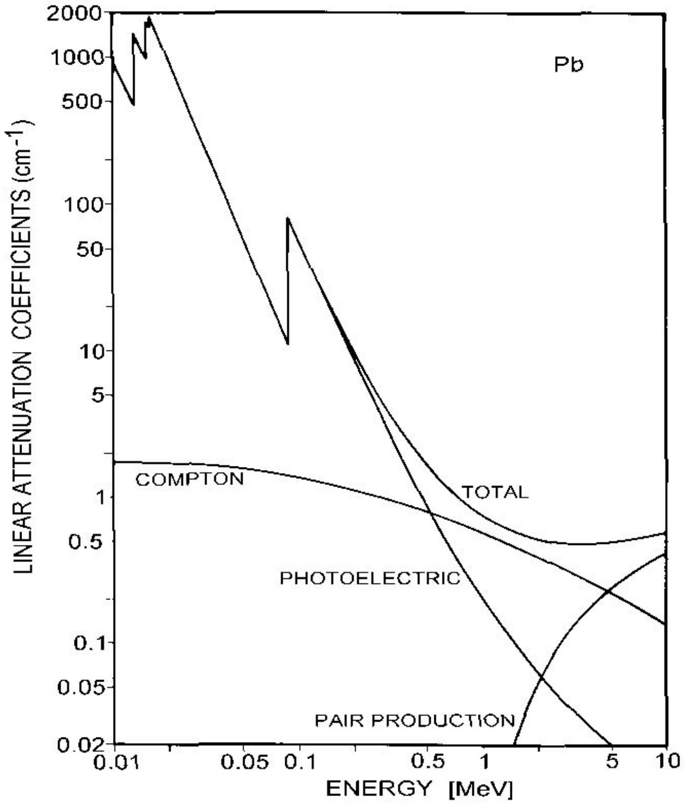

Interaction of low energy photons with matter - 2

Attenuation coefficients for lead and silicon

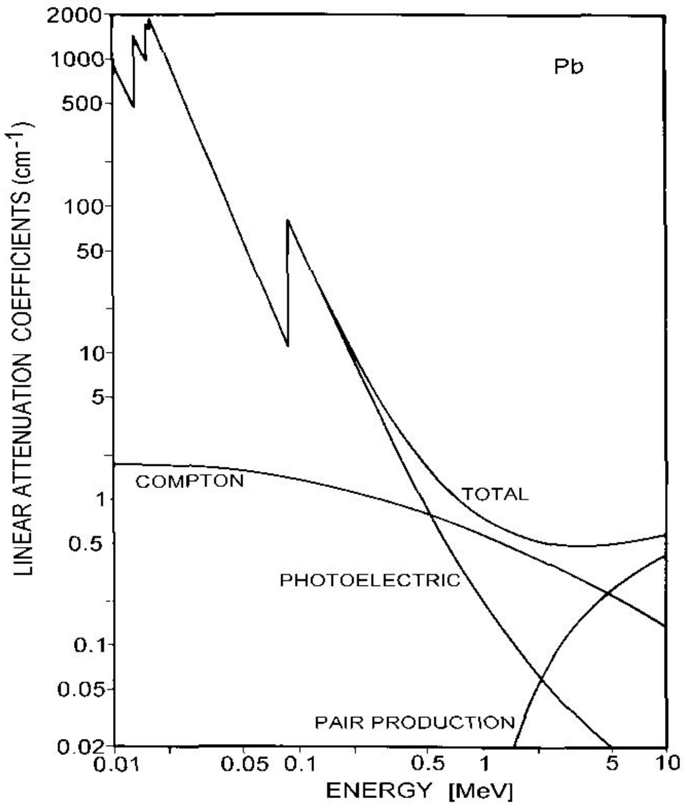

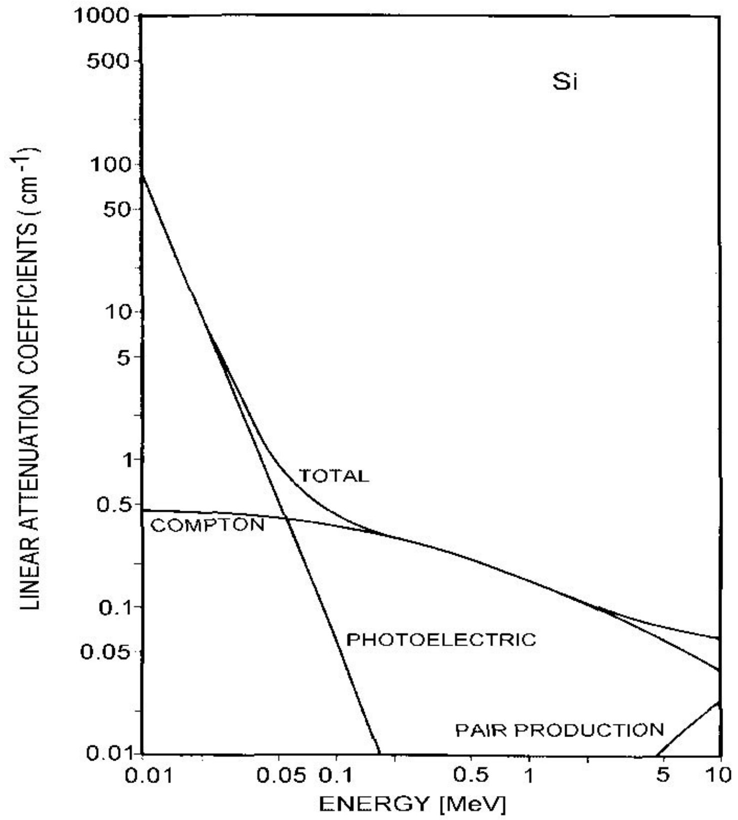

Example of a gamma detector

Scintillator (NaI) with PMT

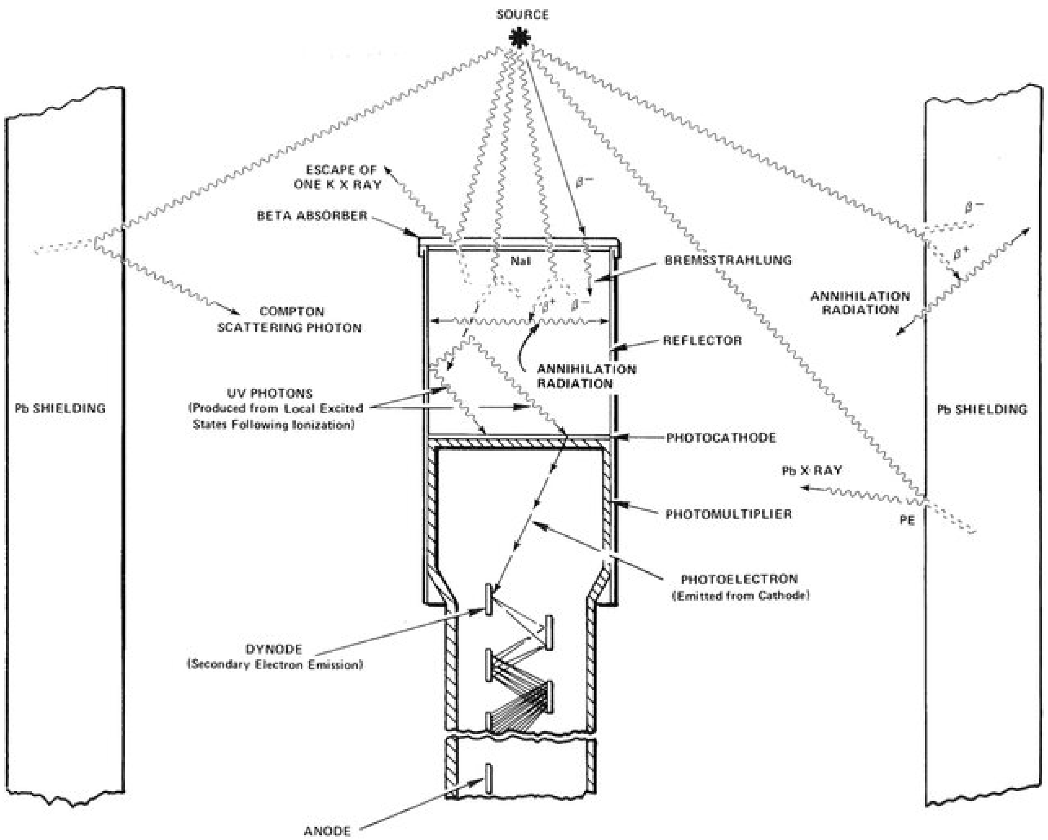

Typical spectra, scintillation counter

Photopeak, Compton edge, escape peak

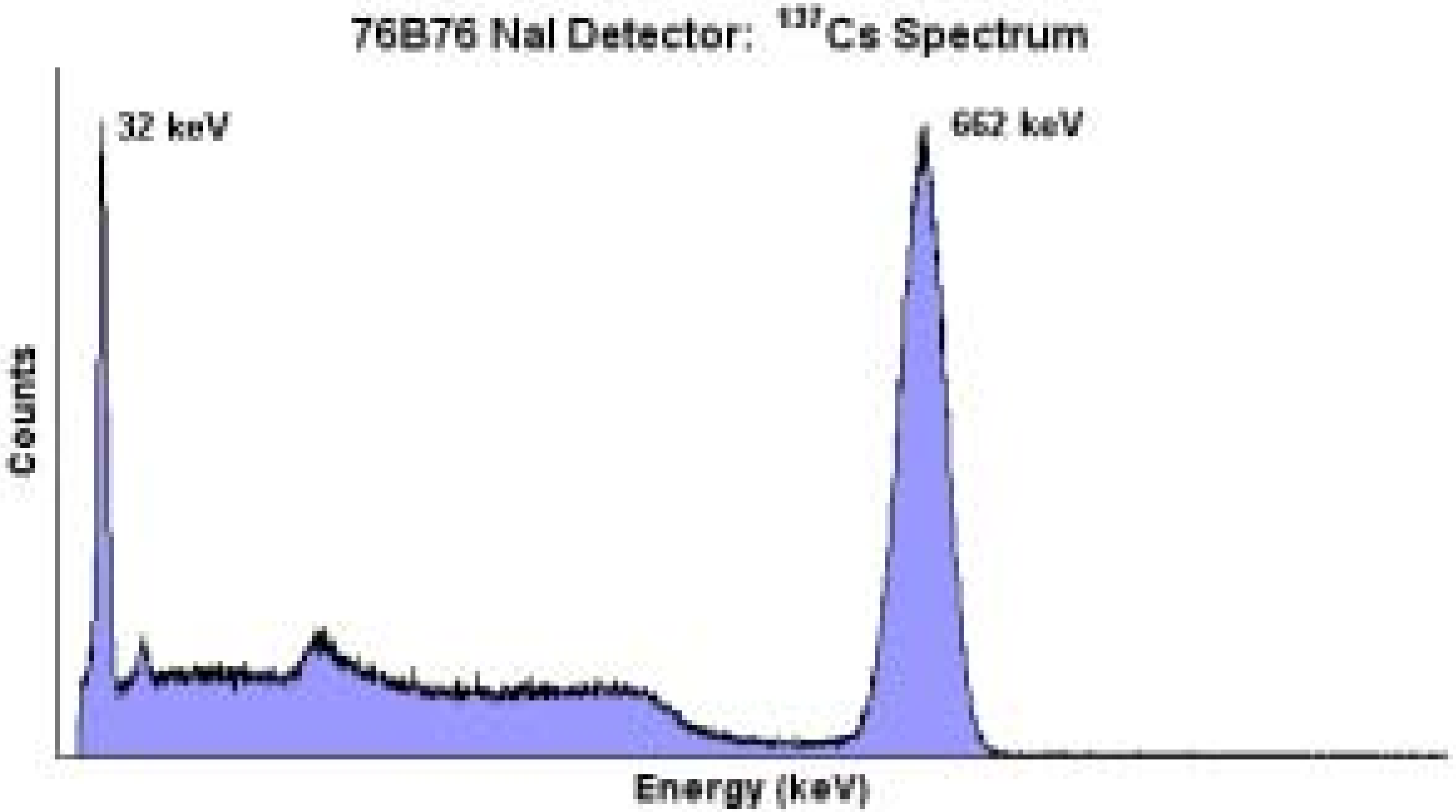

Typical spectra 2

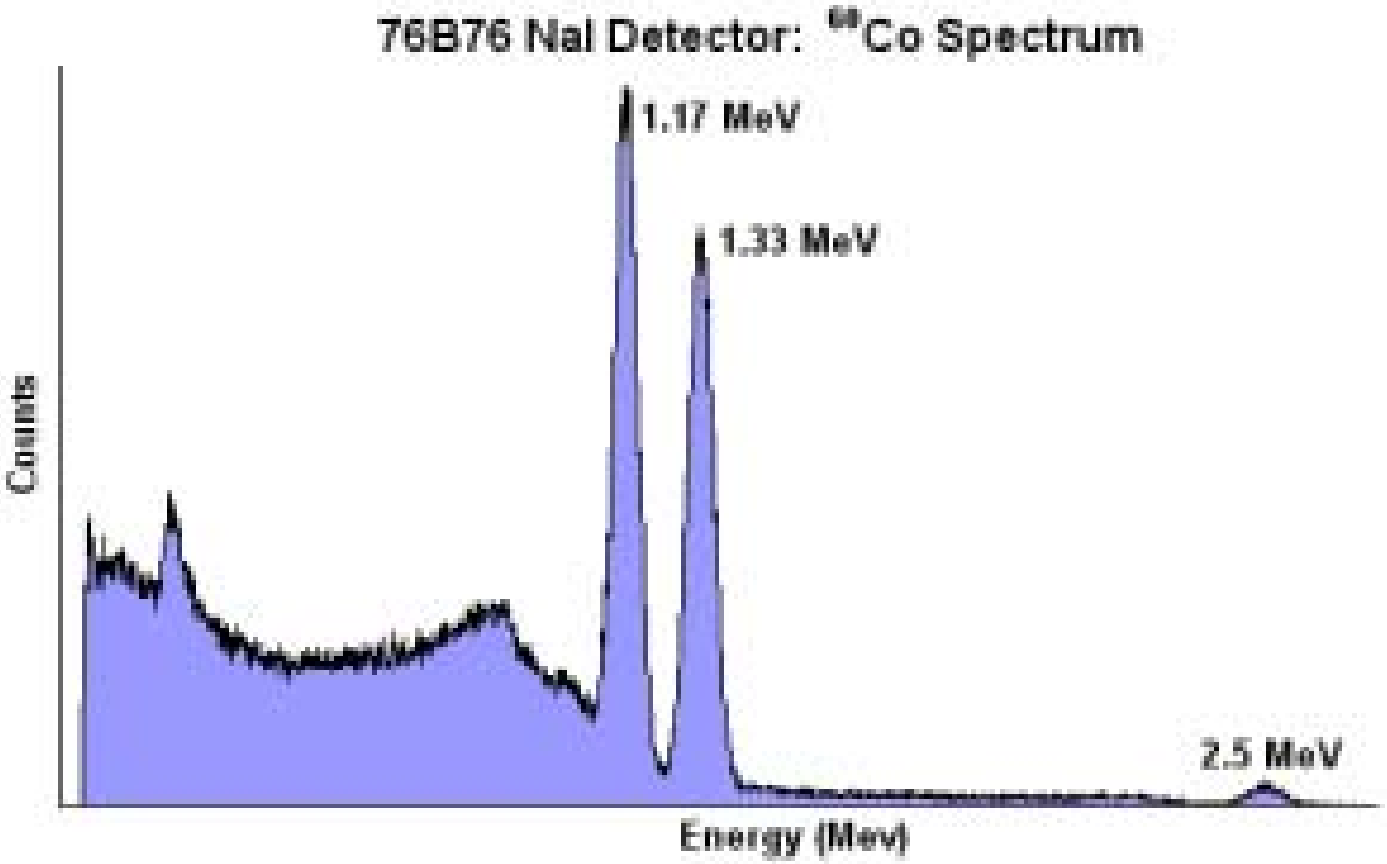

Gamma detection, energy resolution

Resolution: limited by statistics of primary ion-electron pairs (mean ionisation energy W_i)

Naïve: $\sigma(E)/E = (W_i/E)^{1/2}$

Total absorption → total energy fixed:

$\sigma(E)/E = (FW_i/E)^{1/2}$

→ Fano factor F, F=1 for scintillators, 0.2 for gases, and 0.12 semiconductors

Better resolution: exchange scintillator (W_i=30eV) with semiconductor (W_i=3.6eV)

Gamma detection in a semiconductor

Detector:

high-purity Ge

Resolution is superior to the scintillator case – same source as on one of the previous slides

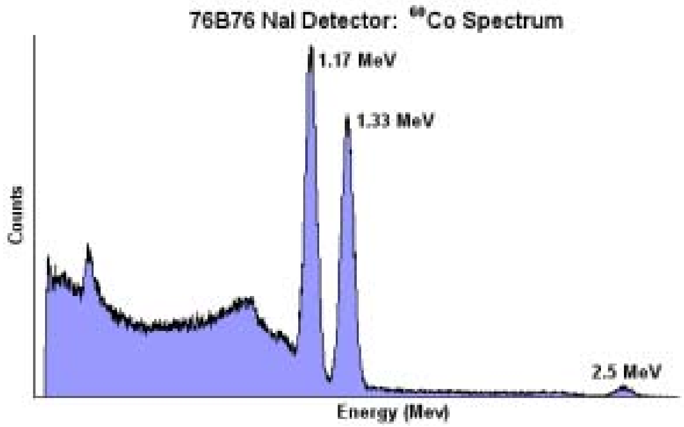

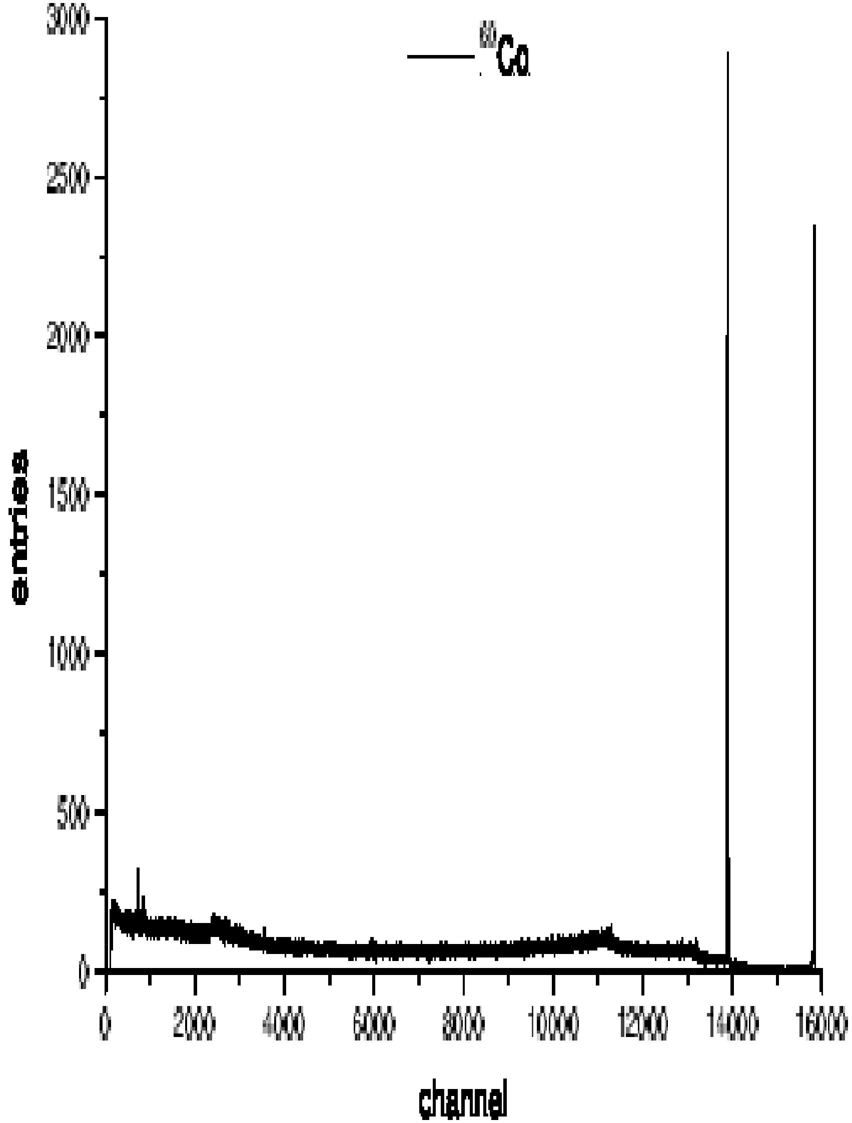

Comparison: radiation spectrum as measured with a Ge (semiconductor) in NaI (scintillation) detector

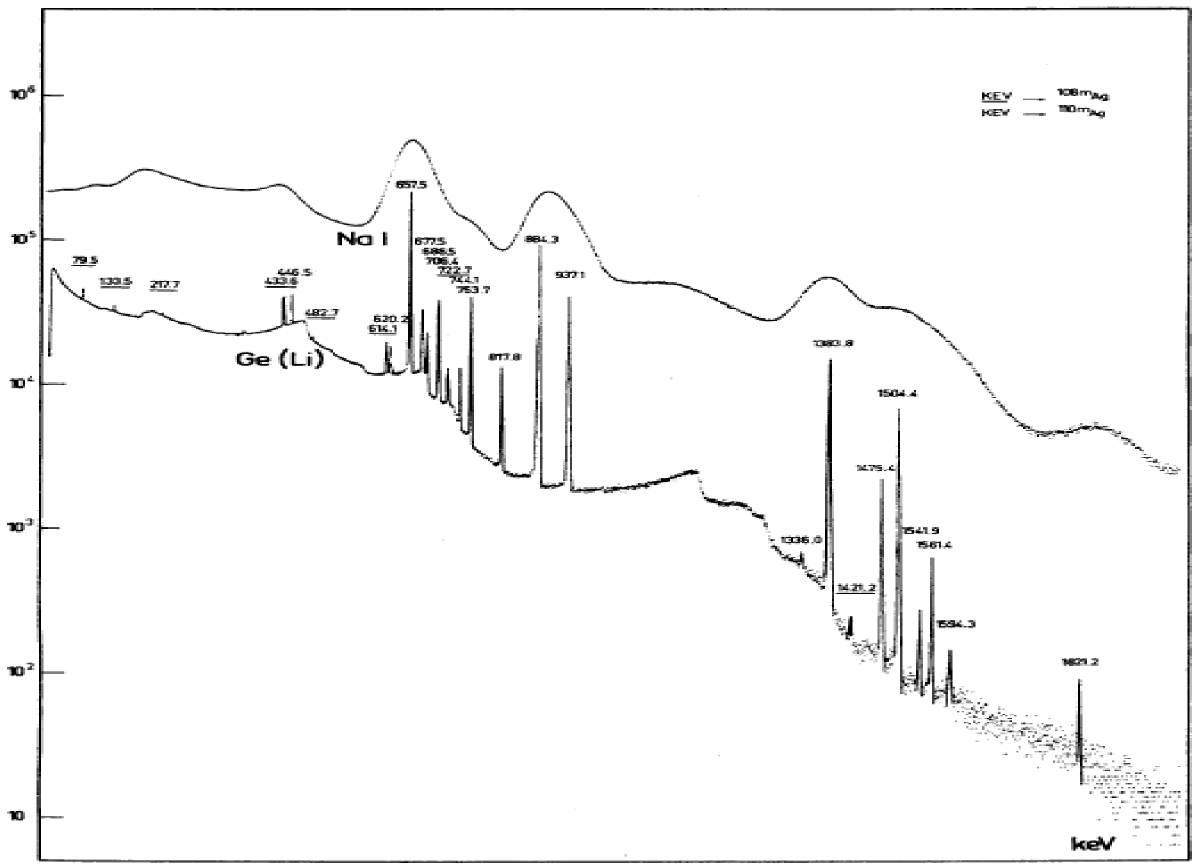

(J.Cl. Philippot, IEEE Trans. Nucl. Sci. NS-17/3 (1970) 446)

Germanium detectors

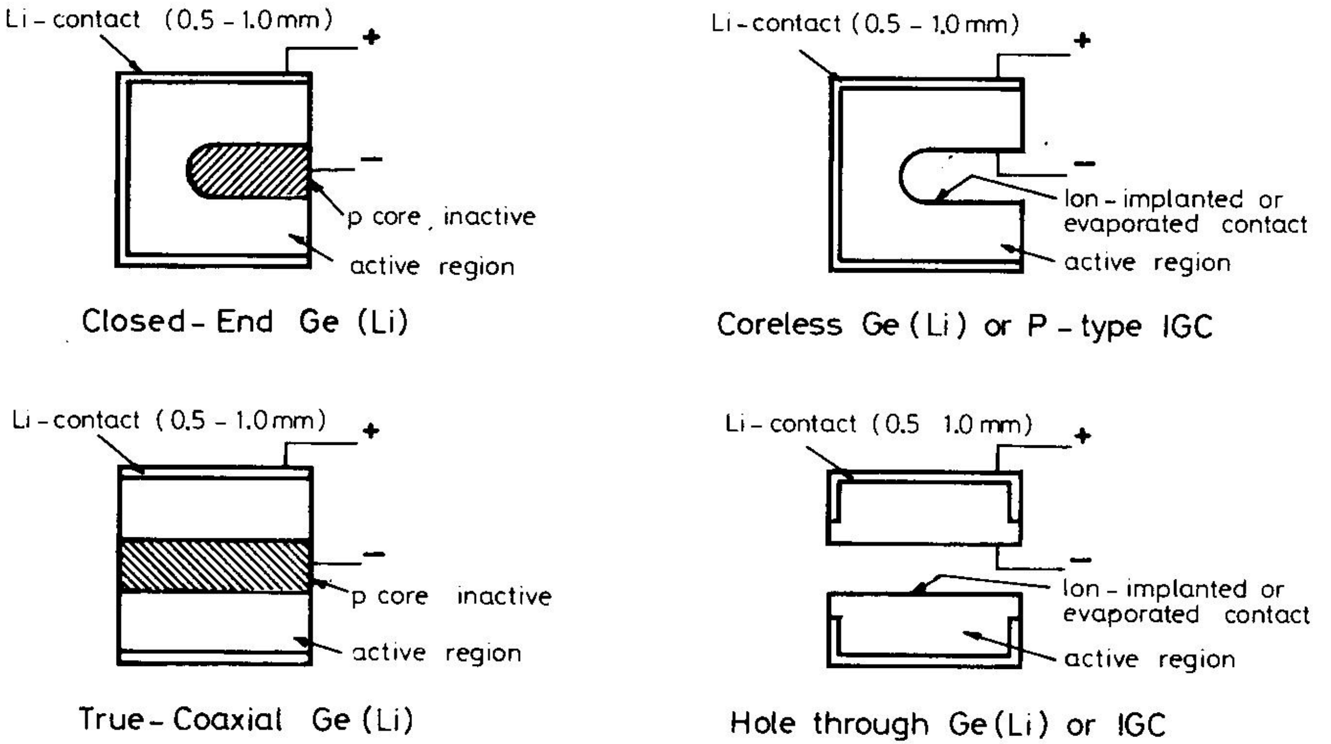

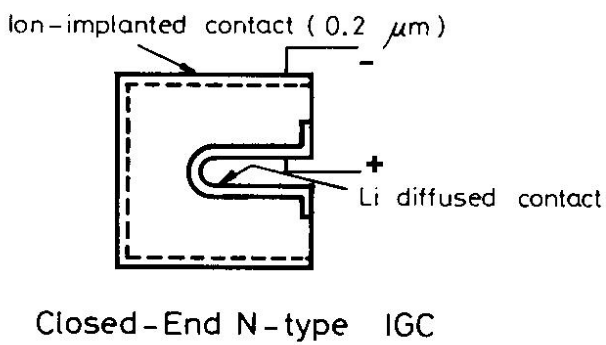

Fig. 10.18. Coaxial configurations for germanium detectors. Lithium is drifted in from the sides leaving an insensitive core (from PGT detector manual [10.21])

Energy resolution of gamma detectors

Depends on the statistical fluctuation in the number of generated electron-hole pairs.

If all energy of the particle gets absorbed in the detector – E_0 (e.g. gamma ray gets absorbed via photoeffect, and the photoelectron is stopped):

on average we get

$$\bar{N}_i = \frac{E_0}{\varepsilon_i}$$

generated pairs

$\varepsilon_i \sim$ 3.6eV for Si
$\sim$ 2.98 eV for Ge

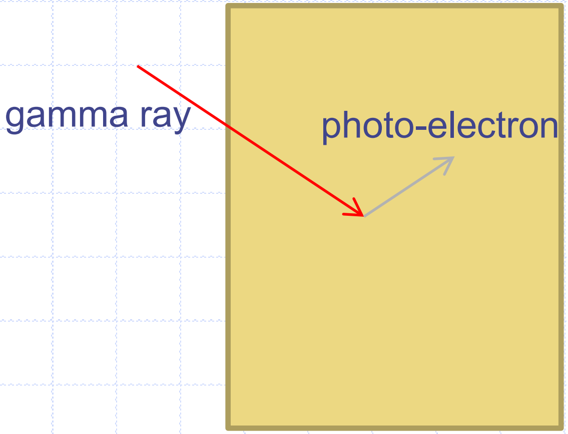

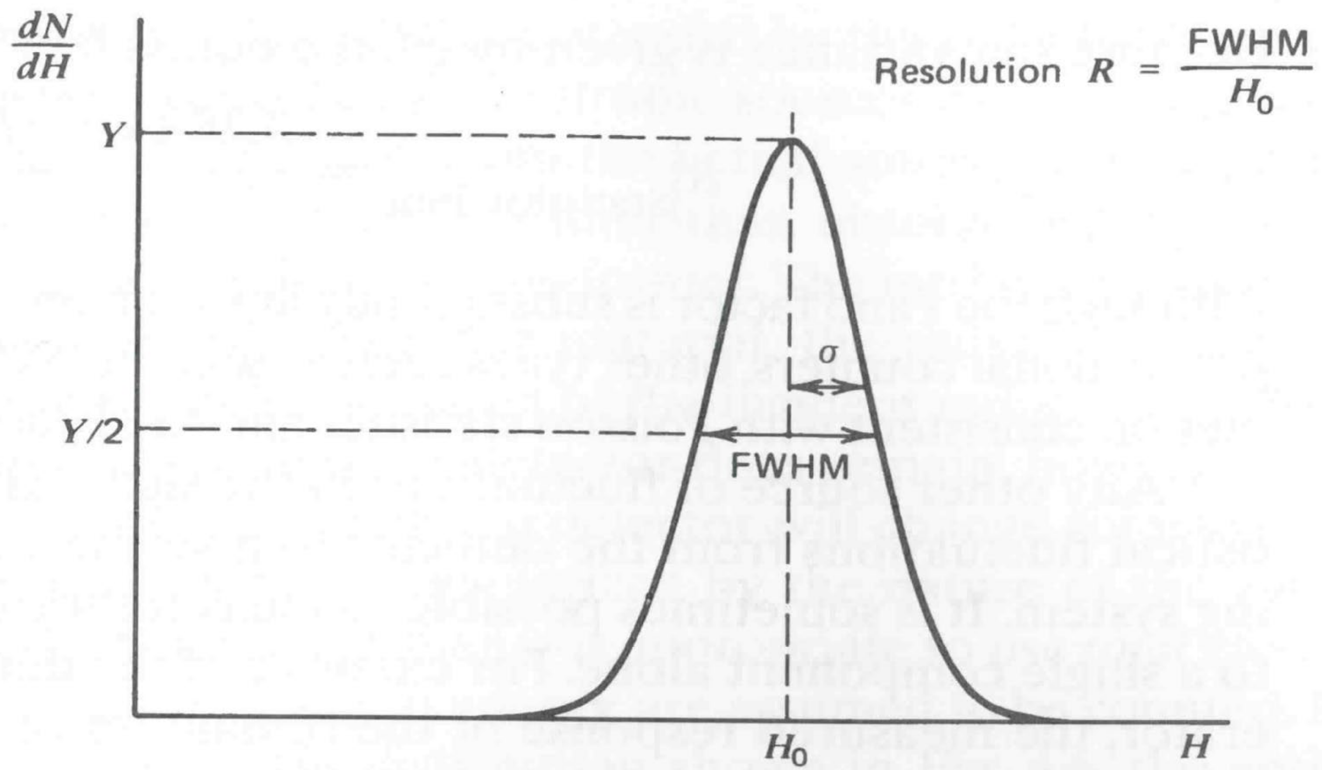

Figure 4.5 Definition of detector resolution. For peaks whose shape is Gaussian with standard deviation σ, the FWHM is given by 2.35σ.

If we have a large number of **independent** events with a small probability (generation of electron-hole pairs) → binominal distribution → Poisson

Standard deviation – r.m.s. (root mean square):

$$\sigma = \sqrt{\bar{N}_i}$$

The measured resolution is actually better than predicted by Poisson statistics

- Reason: the generated pairs e-h are not really independent since there is only a fixed amount of energy available (photoelectron looses all energy).
- Photoelectron looses energy in two ways:

  - pair generation (E_i ~ 1.2 eV per pair in Si)
  - excitation of the crystal (phonons) E_x ~0.04 eV for Si

$\bar{N}_x$ Average number of crystal excitations

$\bar{N}_i$ Average number of generated pairs

$\sigma_x = \sqrt{\bar{N}_x}$ standard deviation

$\sigma_i = \sqrt{\bar{N}_i}$

Since the available energy is fixed (monoenergetic photoelectrons):

$$E_i dN_i = -E_x dN_x \Rightarrow E_i \sigma_i = E_x \sigma_x$$

$$\Rightarrow \sigma_i = \frac{E_x}{E_i}\sqrt{\bar{N}_x}$$

Width of the energy loss distribution

$$E_i\,\bar{N}_i + E_x\,\bar{N}_x = E_0 \Rightarrow \bar{N}_x = \frac{E_0 - E_i\,\bar{N}_i}{E_x}$$

$$\sigma_i = \frac{E_x}{E_i}\sqrt{\frac{E_0 - E_i\,\bar{N}_i}{E_x}} \qquad \text{make use of} \quad \bar{N}_i = \frac{E_0}{\varepsilon}$$

$$\Rightarrow \sigma_i = \sqrt{\bar{N}_i}\sqrt{\frac{E_x}{E_i}\left(\frac{\varepsilon_i}{E_i} - 1\right)} = \sqrt{F\,\bar{N}_i}$$

F Fano factor – improvement in resolution

F ~ 0.1 for silicon

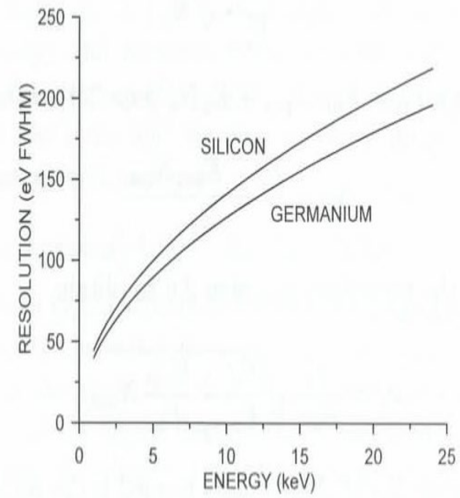

FIG. 2.12. Intrinsic resolution of silicon and germanium detectors *vs.* energy

High resolution gamma detection

Potentially an even better resolution: cryogenic detector, deposited energy is determined by measuring the change in superconductor resistance through a measurement of magnetic flux by a SQUID. Gap: of order meV → an order of magnitude better resolution possible than in semiconductors – in principle. In practice (inhomogenuity of response, electronics noise) comparable to semiconductors.

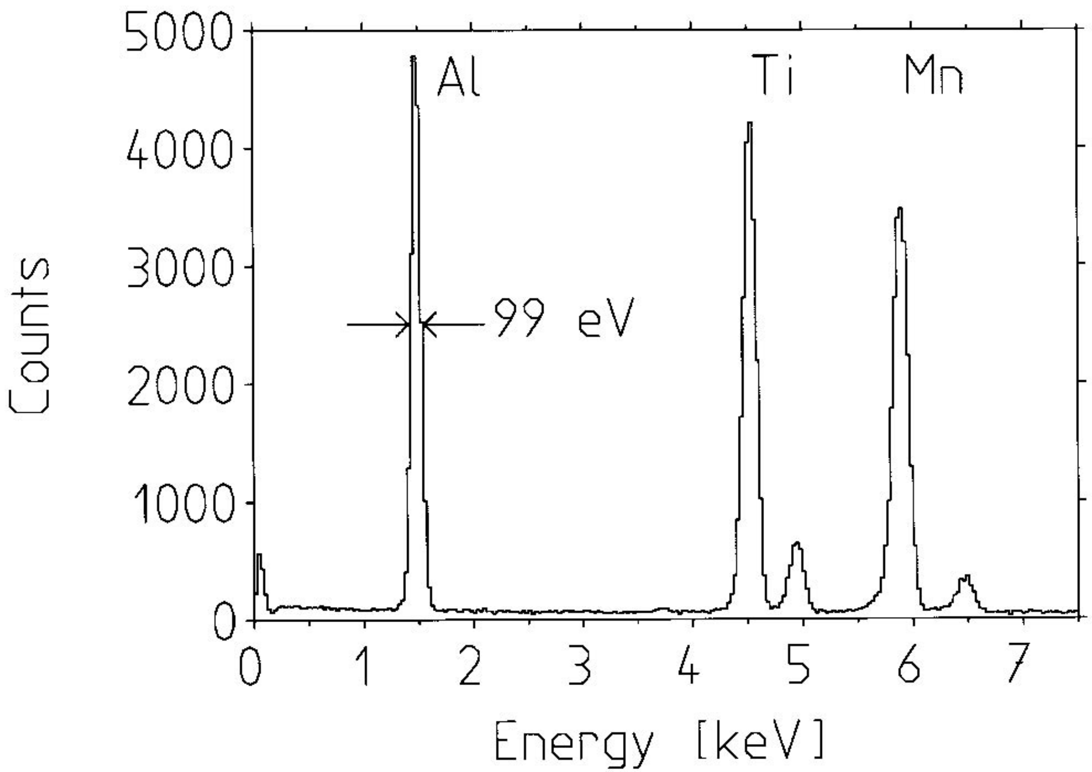

→ At E=5.9 keV: measured

$\sigma(E)/E = 150 / 2.35 / 5900 = 0.011$

Comparison to a semiconductor counter:

$\sigma(E)/E = (F\,W_i/E)^{1/2} = (0.12 \times 3.6/5900)^{1/2} = 0.009$

+ electronics noise etc

→ measured

$\sigma(E)/E = 0.01\text{-}0.02$

Detection of neutrons

In principle similar to the low energy photon detection: again let the neutron interact with the detector medium, and detect charged reaction products

Detection of low energy n: n+nucleus → charged fragments

Three conversion reactions commonly used in detectors:

$^{10}B + n \rightarrow {}^{7}Li^{*} + \alpha + 2.310$ MeV

$^{6}Li + n \rightarrow {}^{3}H + \alpha + 4.78$ MeV

$^{3}He + n \rightarrow {}^{3}H + p + 0.764$ MeV

Because the energy released in these reactions is large compared to the energy of the detected neutron, and the reaction products (which we later detect) carry away this released energy, the information on the neutron energy is lost.

Detection of low energy n: n+nucleus -> charged fragments

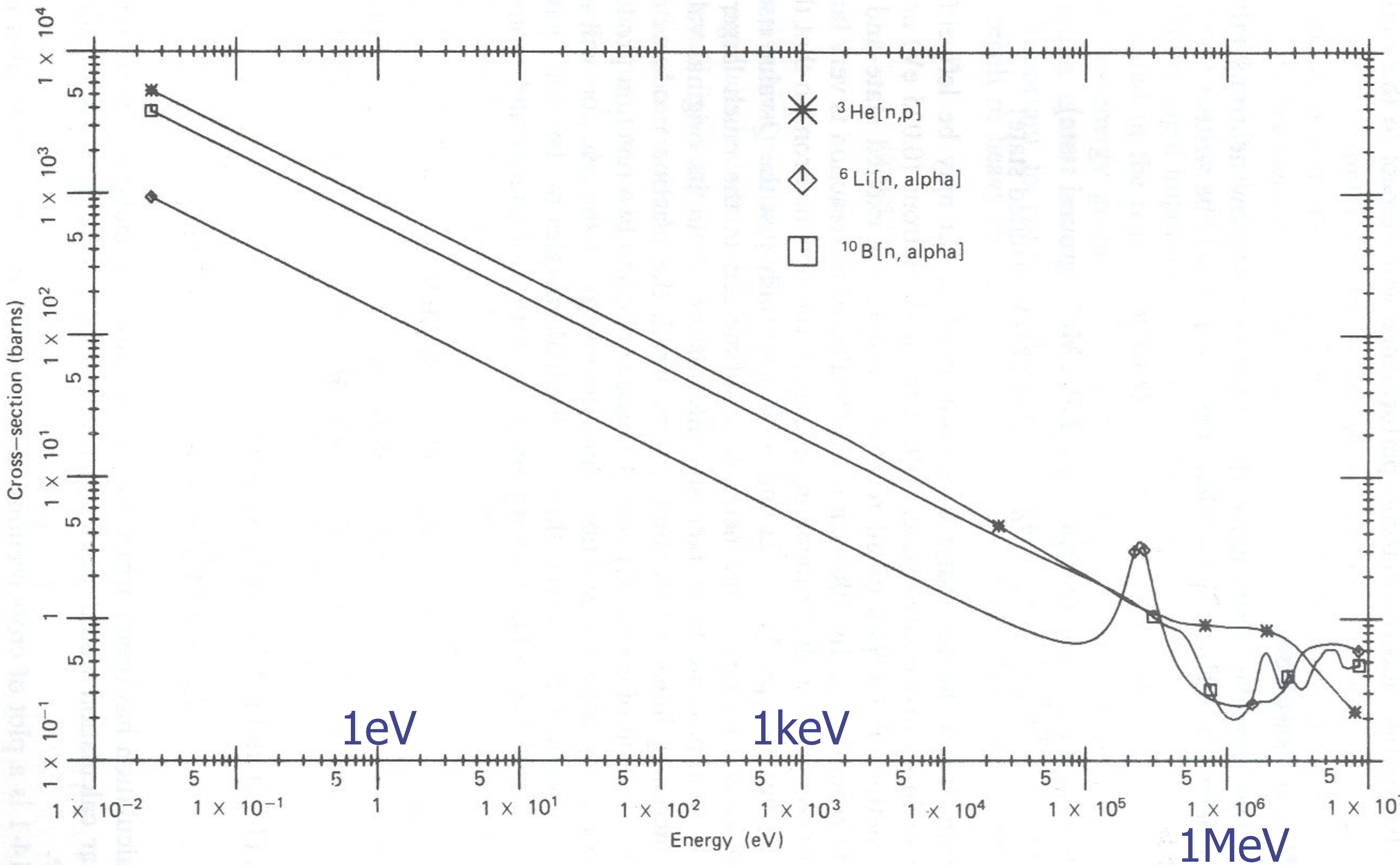

Figure 14-1 Cross section versus neutron energy for some reactions of interest in neutron detection.

Slow neutron detection counters

The boron reaction is employed in BF_3 proportional tubes where boron trifluoride is used as a proportional gas. The BF_3 gas is usually enriched in ^{10}B, and it has to be used at lower absolute pressures between 0.5 and 1.0 atm in order to get a good performance as a proportional gas.

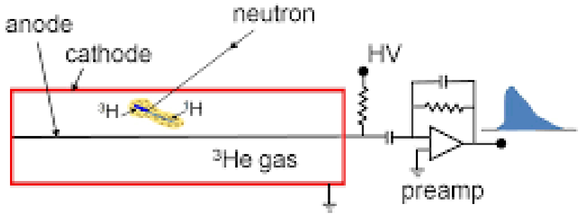

In a similar way, ^3He is used as a conversion target and proportional gas in the ^3He proportional counter. Due to the lower energy released in the $^3He(n,p)$ reaction, the discrimination of gamma rays is more difficult than with BF_3 counters, since secondary electrons only deposit a small amount of energy in the gas.

Slow neutrons (T<0.5eV): typical spectrum

$^{10}B + n \rightarrow {}^{7}Li^{*} + \alpha + 2.310\ MeV$

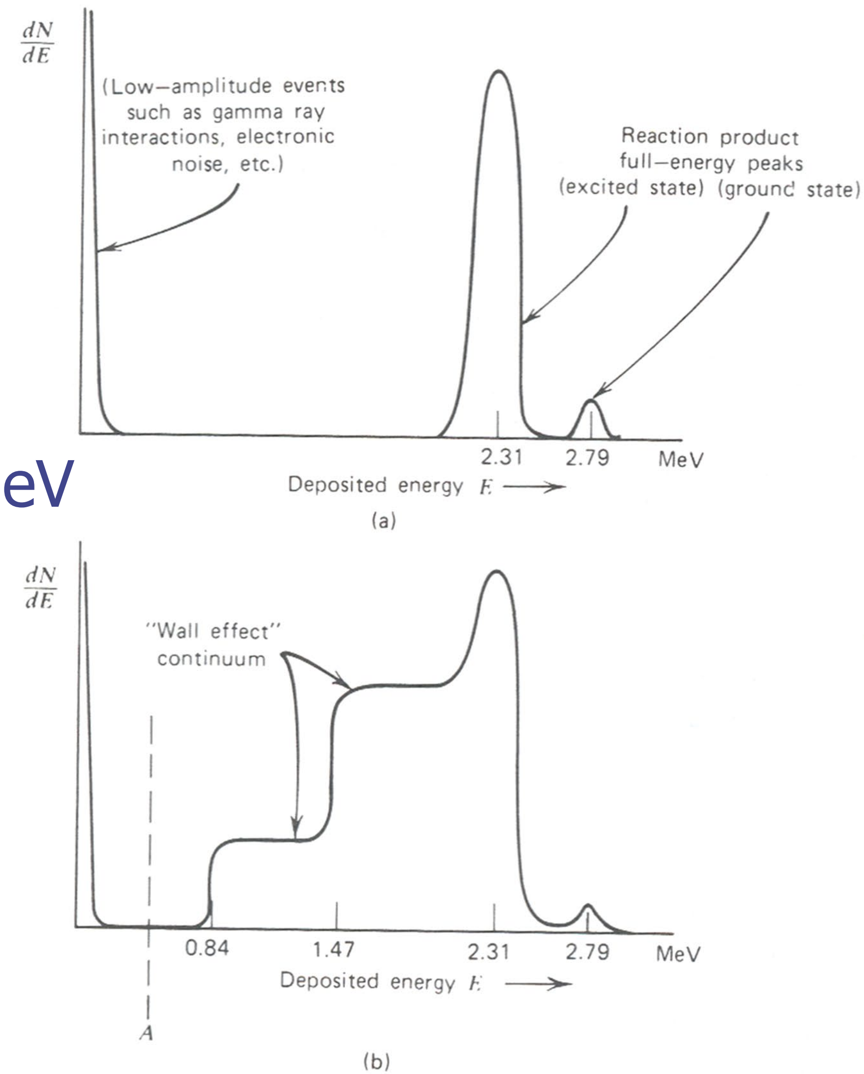

Figure 14-3 Expected pulse height spectra from BF_3 tubes. (a) Spectrum from a large tube in which all reaction products are fully absorbed. (b) Additional continuum due to the wall effect.

Neutron detectors with Li

^{6}Li is usually used in scintillators, e.g. lithium iodide, which is chemically similar to sodium iodide. Due to the density of enriched $^{6}LiI(Eu)$ crystals, a 10 mm thick detector is almost 100% efficient for neutrons ranging from thermal energies up to about 0.5 eV.

Lithium is also incorporated in scintillating glass matrices. Lithium glass scintillators are used in time-of-flight measurements due to their relatively fast time response of less that 100 ns. This type of detector, however, is more commonly used in the detection of neutrons with intermediate energies.

Neutrons with T around 1MeV

Cross section much lower than for thermal neutrons – employ a moderator where neutrons loose energy after elastic scattering – most efficient if it has a large fraction of hydrogen (e.g. organic compounds like polyethylene and paraffin)

Neutron detection: combination of several methods

- ^3He
- BF_3
- moderator
- shield

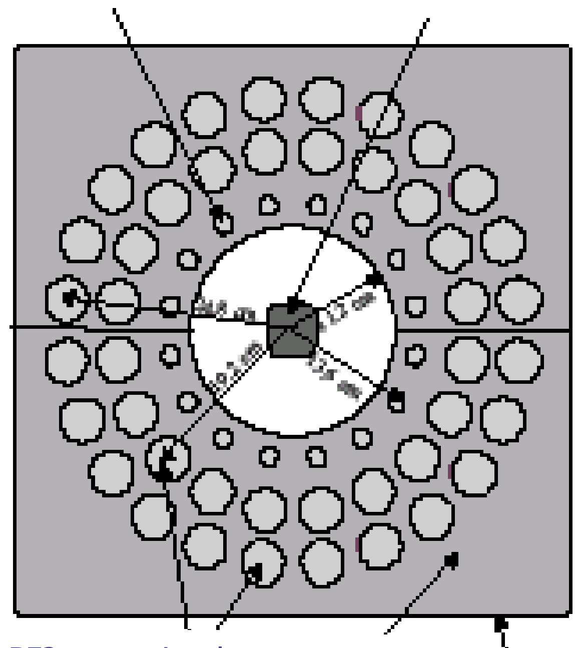

Discrimination against gamma rays

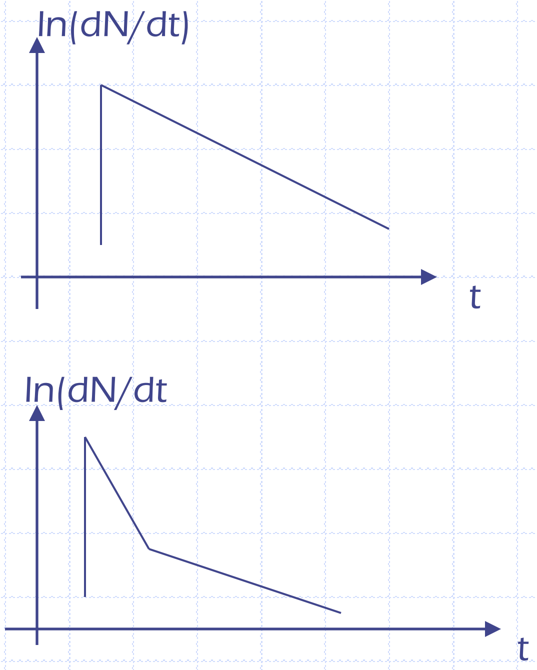

Some scintilators have two decay constants

$$dN/dt = A\exp(-t/\tau_1) + B\exp(-t/\tau_2)$$

→ In such scintilation materials the ratio of the two components depends on the particle type since the light yield of the two components depends on dE/dx, which, in turn, depends on the particle type.

→

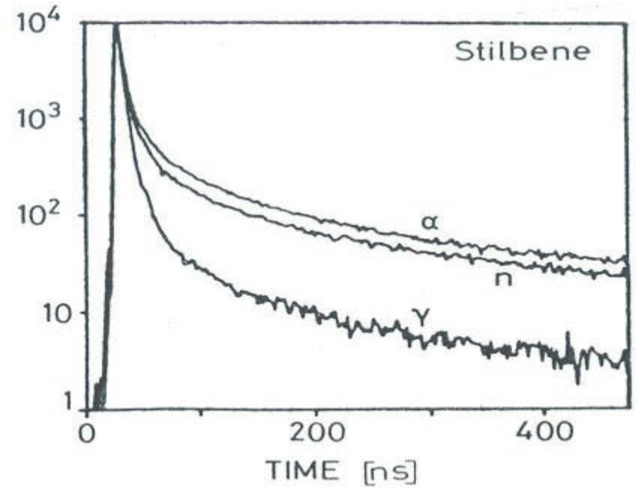

Fig. 7.11. Pulse shape of stilbene light for alpha particles, neutrons, and gamma rays (from *Lynch* [7.71]; picture © 1975 IEEE)

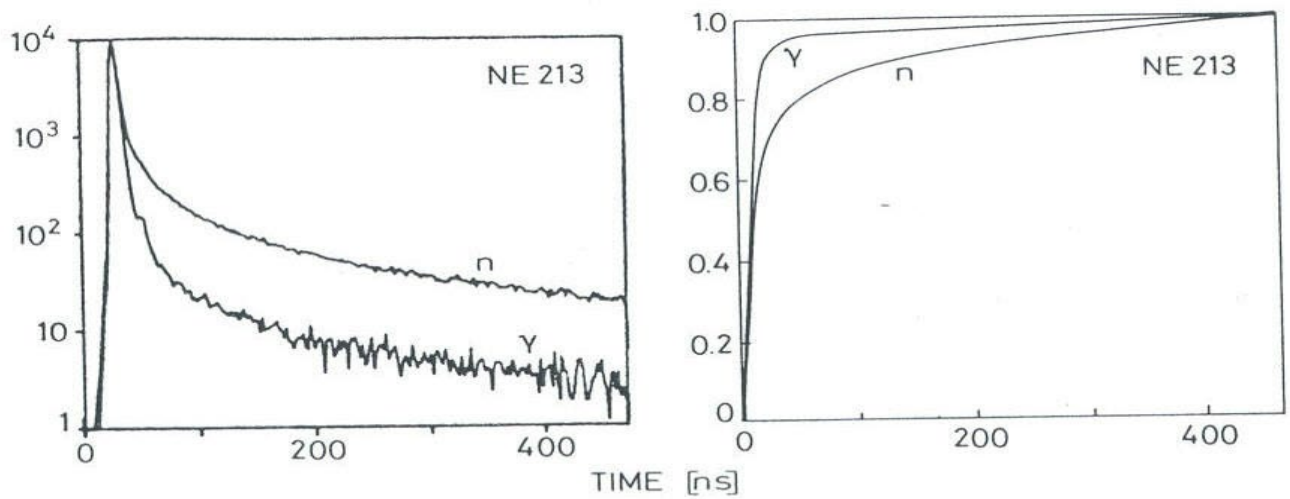

Fig. 7.12. Pulse shape differences of NE 213 liquid scintillator light for neutrons and gamma rays. The time integral of the light pulses is also shown. A discrimination between these radiations may be obtained by measuring the time it takes for the integrated pulse to reach a certain fixed level (from *Lynch* [7.17]; picture © 1975 IEEE)

Medium energy neutrons (=fast n)

For neutrons of even higher energies ($20MeV<T<1GeV$) the use of a moderator is unpractical, furthermore, moderator based detectors are slow and cannot be used for time measurements.

The most common method to detect fast neutrons is based on elastic scattering of neutrons on light nuclei, resulting in a recoil nucleus. This is also the principle of proton recoil scintillators. Fast neutrons incident on a hydrogen-containing scintillator will scatter elastically and give rise to recoil protons ranging in energy up to the full neutron energy. The energy of the recoil protons is then deposited in the scintillator and converted to fluorescence.

A large variety of hydrogen-containing scintillators is available: organic crystals (anthracene, stilbene), liquid scintillators (organic scintillators in an organic solvent), and plastic scintillators (organic scintillators in a polymerized hydrocarbon)

High energy neutrons

For neutrons with several GeV energy: hadron calorimeters $\rightarrow$ lecture 'Energy measurements'

Neutrino detection

Use inverse beta decay

$\nu_e + n \rightarrow p + e^-$

$\bar{\nu}_e + p \rightarrow n + e^+$

$\nu_\mu + n \rightarrow p + \mu^-$

$\bar{\nu}_\mu + p \rightarrow n + \mu^+$

$\nu_\tau + n \rightarrow p + \tau^-$

$\bar{\nu}_\tau + p \rightarrow n + \tau^+$

However: cross section is very small!

$6.4\ 10^{-44}\ cm^2$ at 1MeV

Probability for interaction in 100m of water = $4\ 10^{-16}$

Neutrino detection - history

$\bar{\nu}_e + p \rightarrow n + e^+$

$e^+ + e^- \rightarrow \gamma\,\gamma$

$n + Cd \rightarrow Cd^* \rightarrow Cd + \gamma$

Reines-Cowan experiment

$\nu_e + n \rightarrow p + e^-$

$\nu_e + {}^{37}Cl \rightarrow {}^{37}Ar^* + e^-$

${}^{37}Ar^* \rightarrow {}^{37}Ar + \gamma$

Davies experiment

Electron neutrino detected in a bubble chamber

Electron neutrino produces an electron, which then starts a shower. Tracks of the shower are curved in the magnetic field.

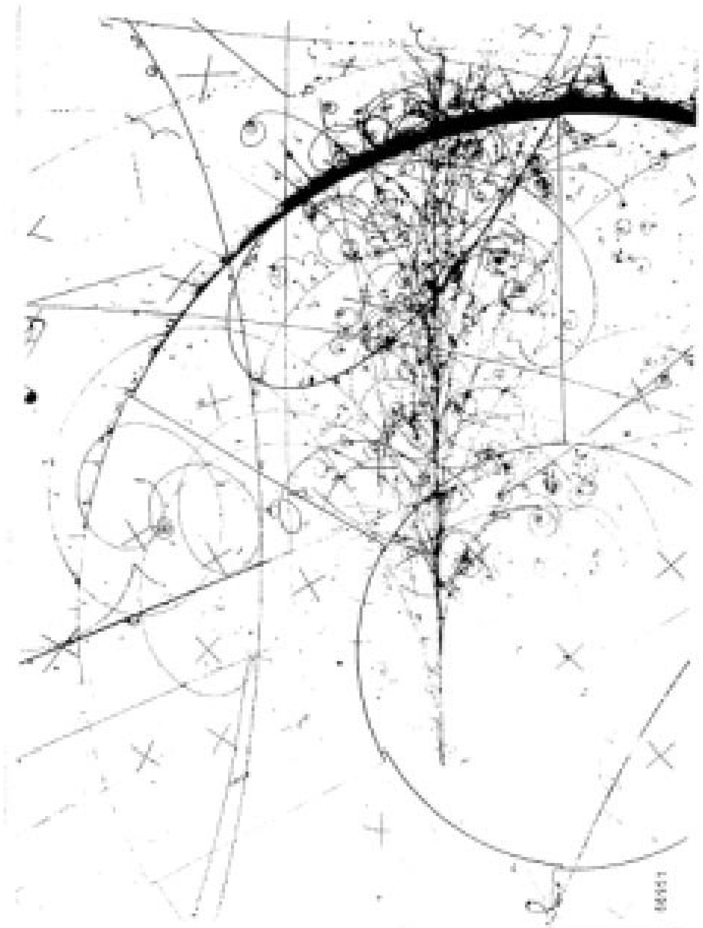

ν_e

Which type of neutrino?

Identify the reaction product, e,μ,τ, and its charge.

Water detectors (e.g. Superkamiokande)

muon: a sharp Cherenkov ring

electron: Cherenkov ring is blurred (e.m. shower development)

tau: decays almost immediately – after a few hundred microns to one or three charged particles

High energy neutrinos

Interaction cross section:

Neutrinos:

$0.67\ 10^{-38}$ E/1GeV cm^2 per nucleon

Antineutrinos:

$0.34\ 10^{-38}$ E/1GeV cm^2 per nucleon

At 100 GeV, still 11 orders below the proton-proton cross section

Superkamiokande: an example of a neutrino detector

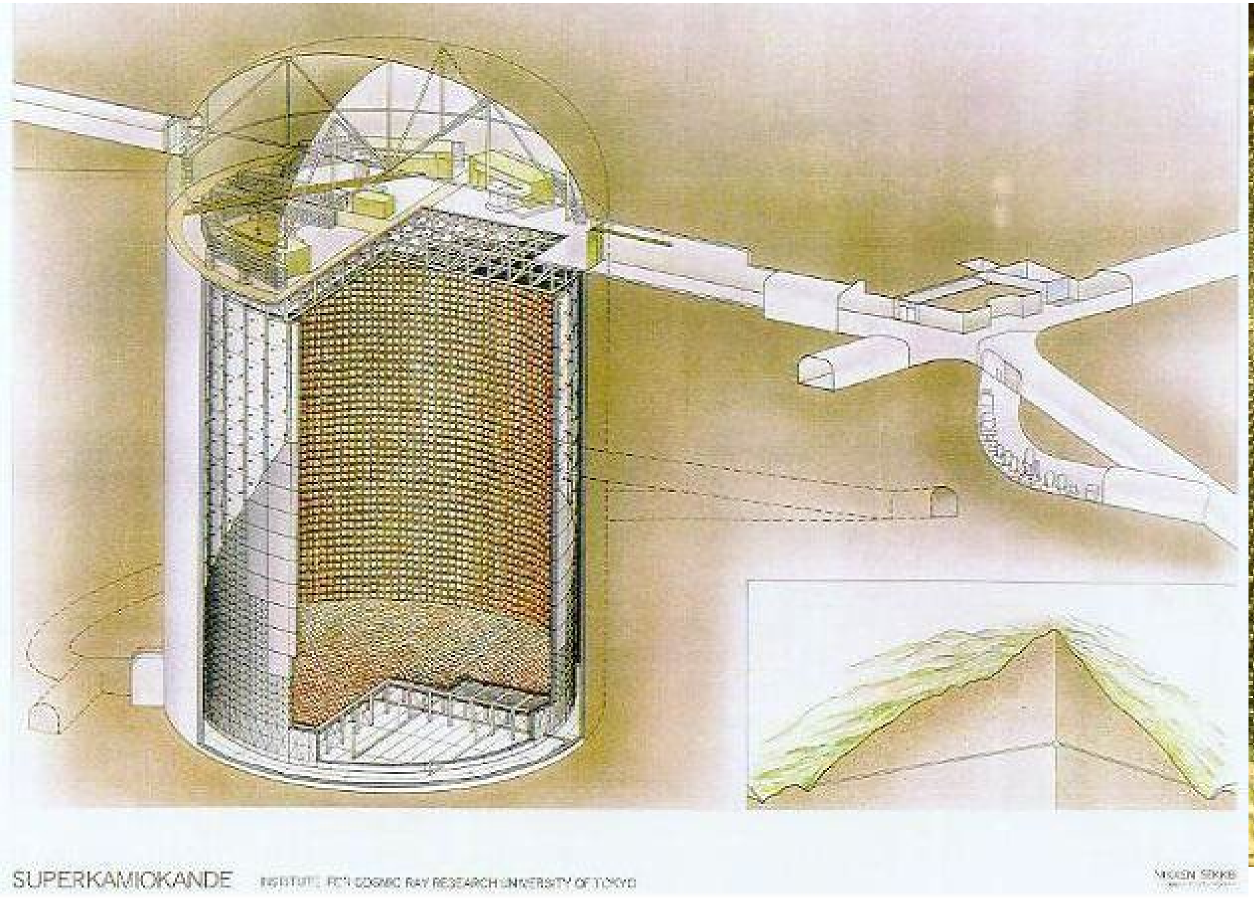

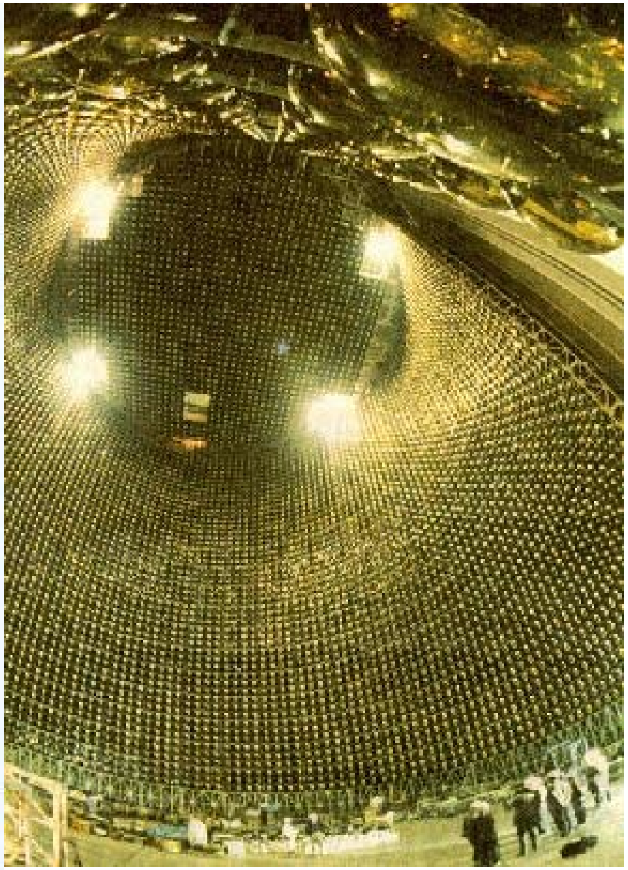

Superkamiokande: an example of a neutrino detector

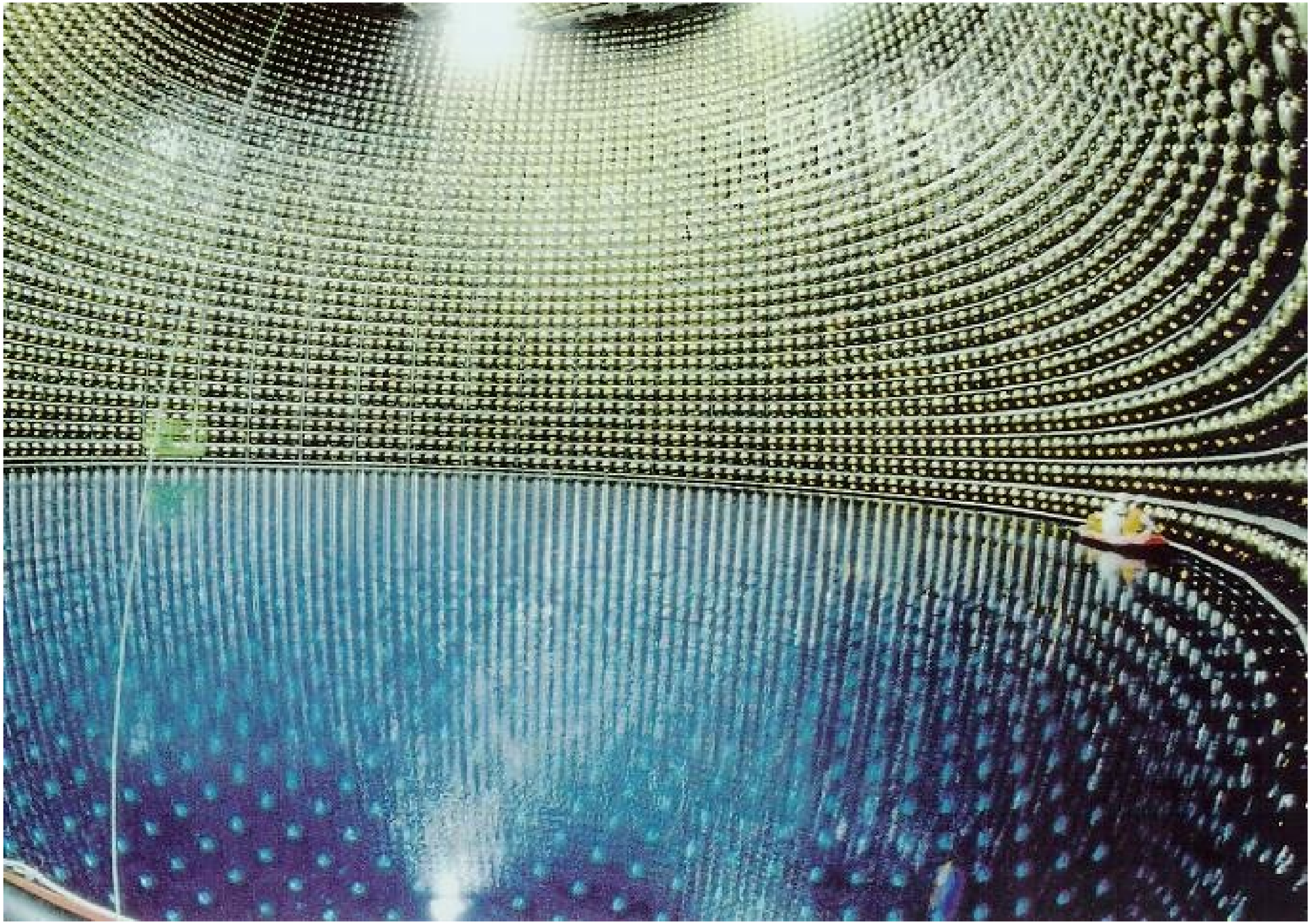

Superkamiokande: detection of Cherenkov photons

Light sensors: HUGE photomultipler tubes

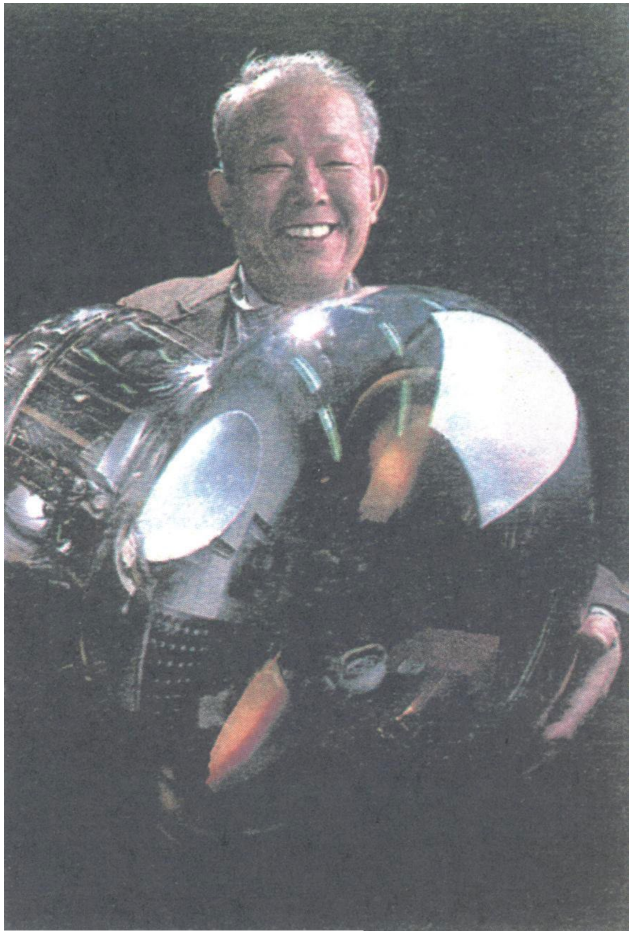

M. Koshiba

Superkamiokande: an example of a neutrino detector

Kamiokande Detector ("Kamioka Nucleon Decay Experiment"):
1000 8″ PMTs in 4500-tonne pure water target

Limits on proton decay,
First detection of neutrinos from supernova,
11 events from SN in Large Magellanic Cloud, Feb 23, 1987

Super-Kamiokande Detector
11000 20″ + 1900 8″ PMTs in 50000-tonne pure water target

- Operation since 1996, measurements of neutrino oscillations via up down asymmetry in atmospheric ν rate
- Solar ν flux (all types) 45% of that expected
- Accident November 2001: loss of 5000 20″ PMTs, now replaced

Superkamiokande: detection of electrons and muons

How to detect muons or electrons? Again through Cherenkov radiation, this time in the water container. Neutrino turns into an electron or muon.

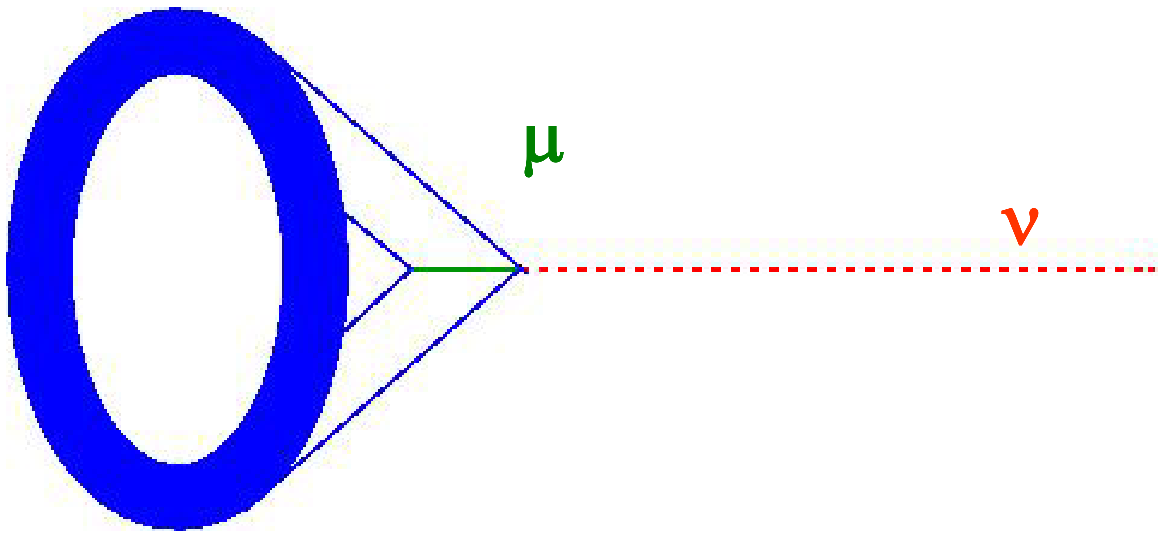

Muons and electrons emit Cherekov photons
→ ring at the container wals

- Muon ring: sharp edges
- Electron ring: blurred image (bremstrahlung)

Muon vs electron

Cherenkov photons from a muon track:

Example: 1GeV muon neutrino

Track length of the resulting muon: $L=E/(dE/dx)= =1GeV/(2MeV/cm)=5m$

→ a well defined “ring” on the walls

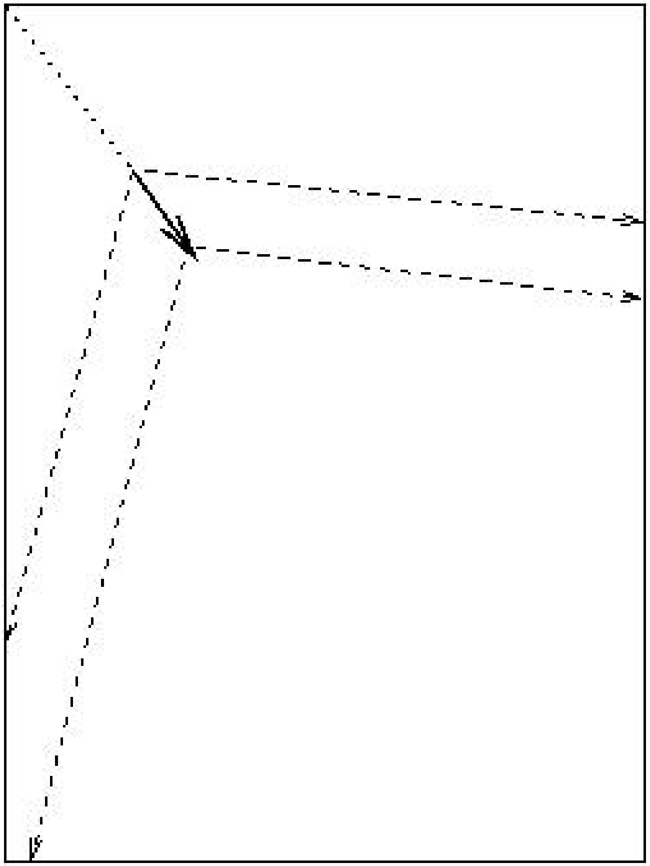

Superkamiokande: muon event

Muon ‘ring’ as seen by the photon detectors

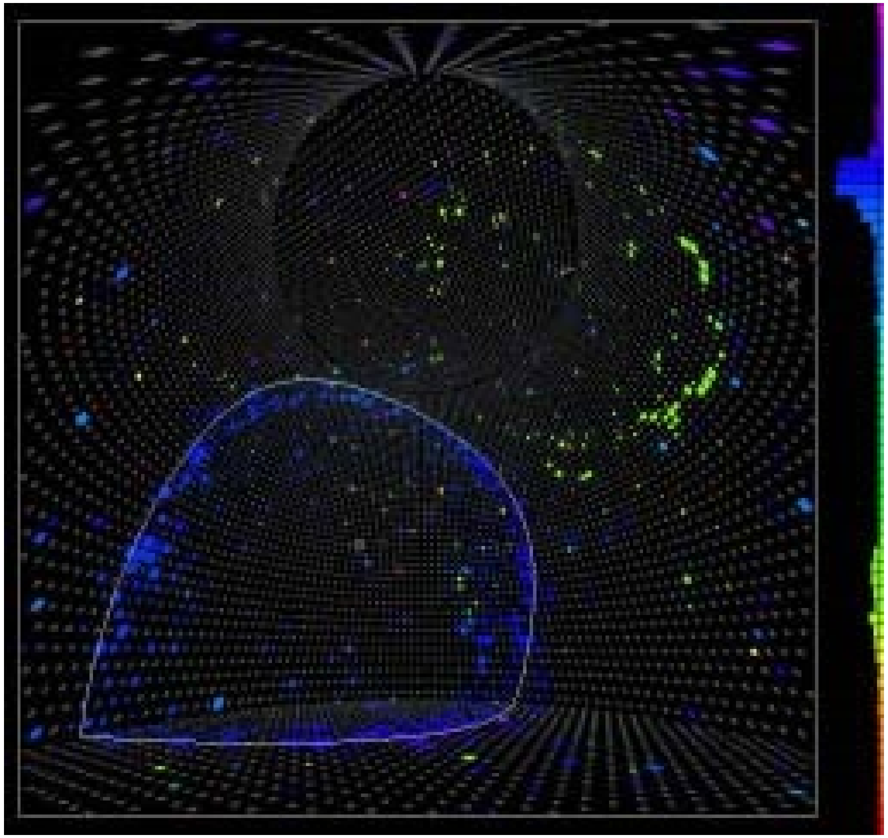

Muon event: photon detector cillinder walls

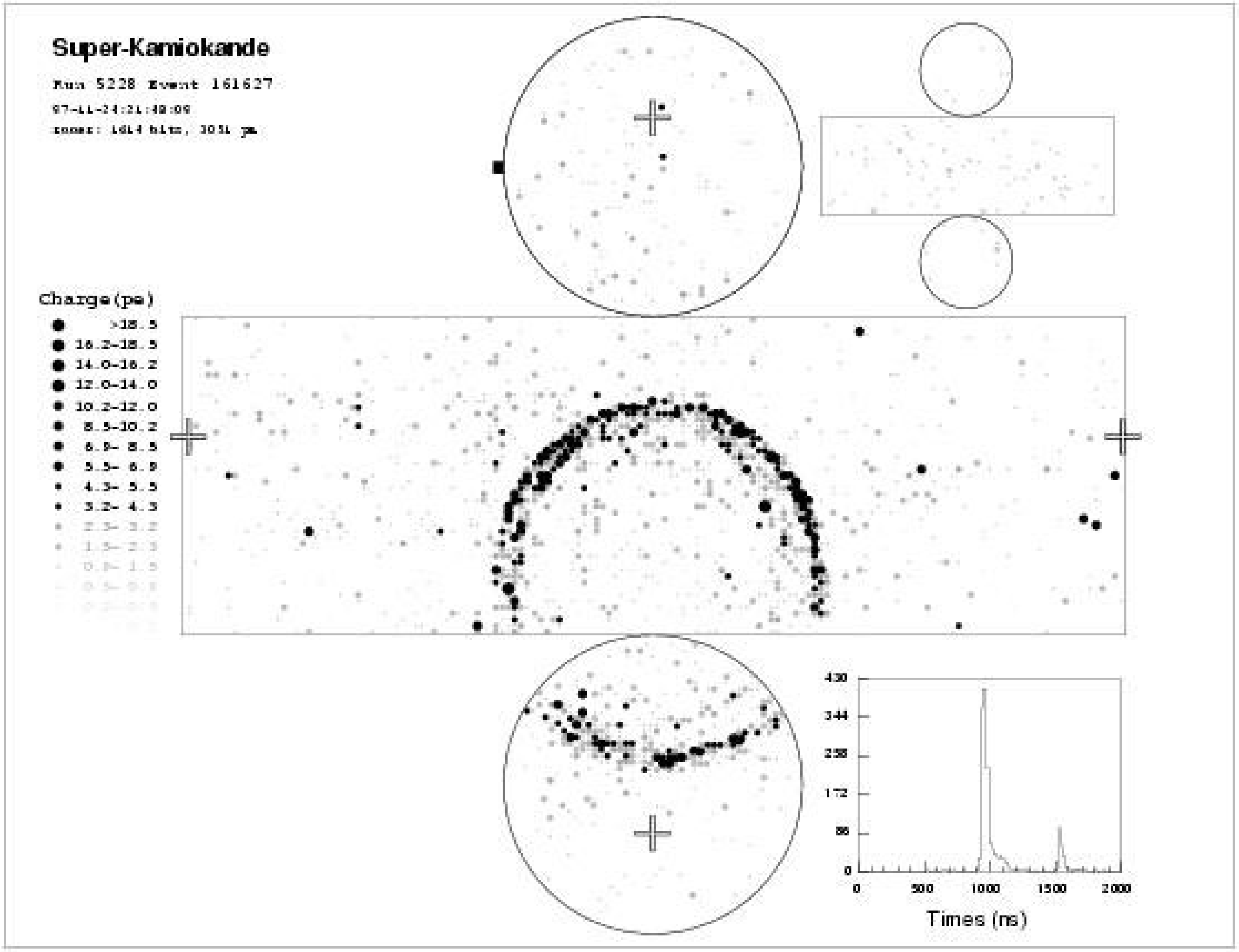

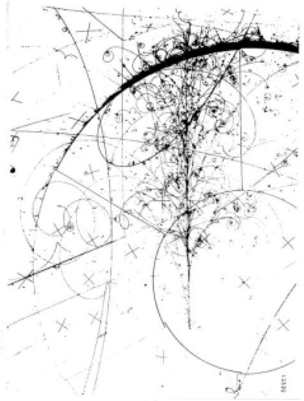

Cherenkov photons from an electron track

- Electron starts a shower!
- Cherenkov photons from an electron generated shower
- Example: 1GeV el. neutrino
- Shower length:
- $L=X_0*\log_2(E/E_{crit})= 36cm*\log_2(1GeV/10MeV) =2.5m$

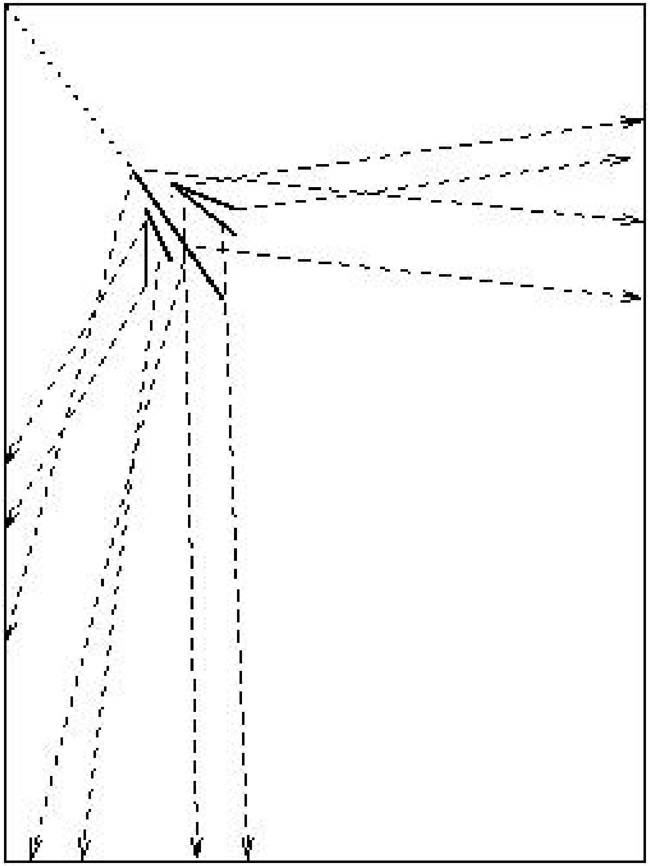

- Shower particles are not parallel to each other
- -> a blurred, less well defined "ring" on the walls

Electron event: blurred ring

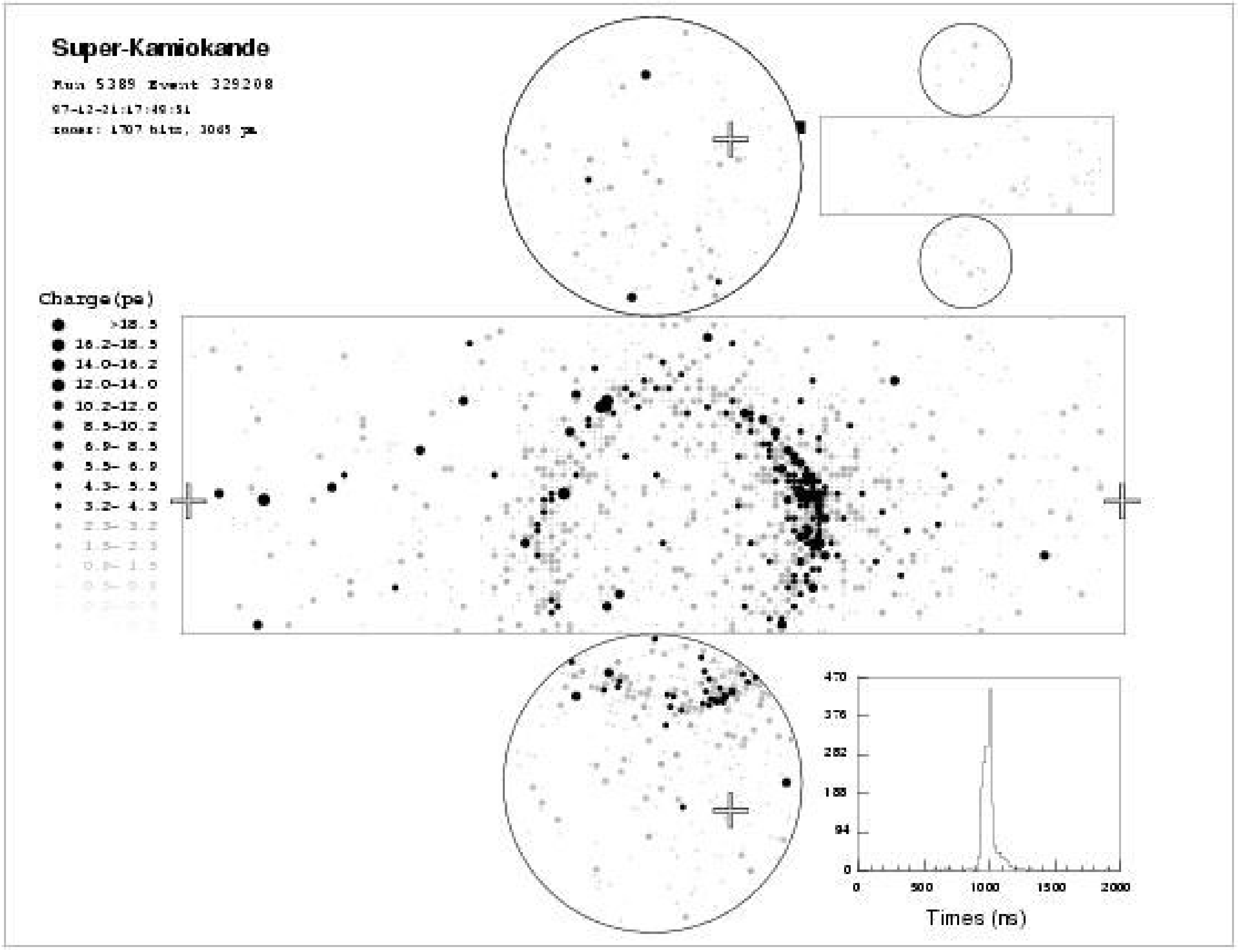

Detection of τ neutrinos

$\nu_\tau + n \rightarrow p + \tau^-$

$\tau^- \rightarrow \mu^- \bar{\nu}_\mu \nu_\tau$

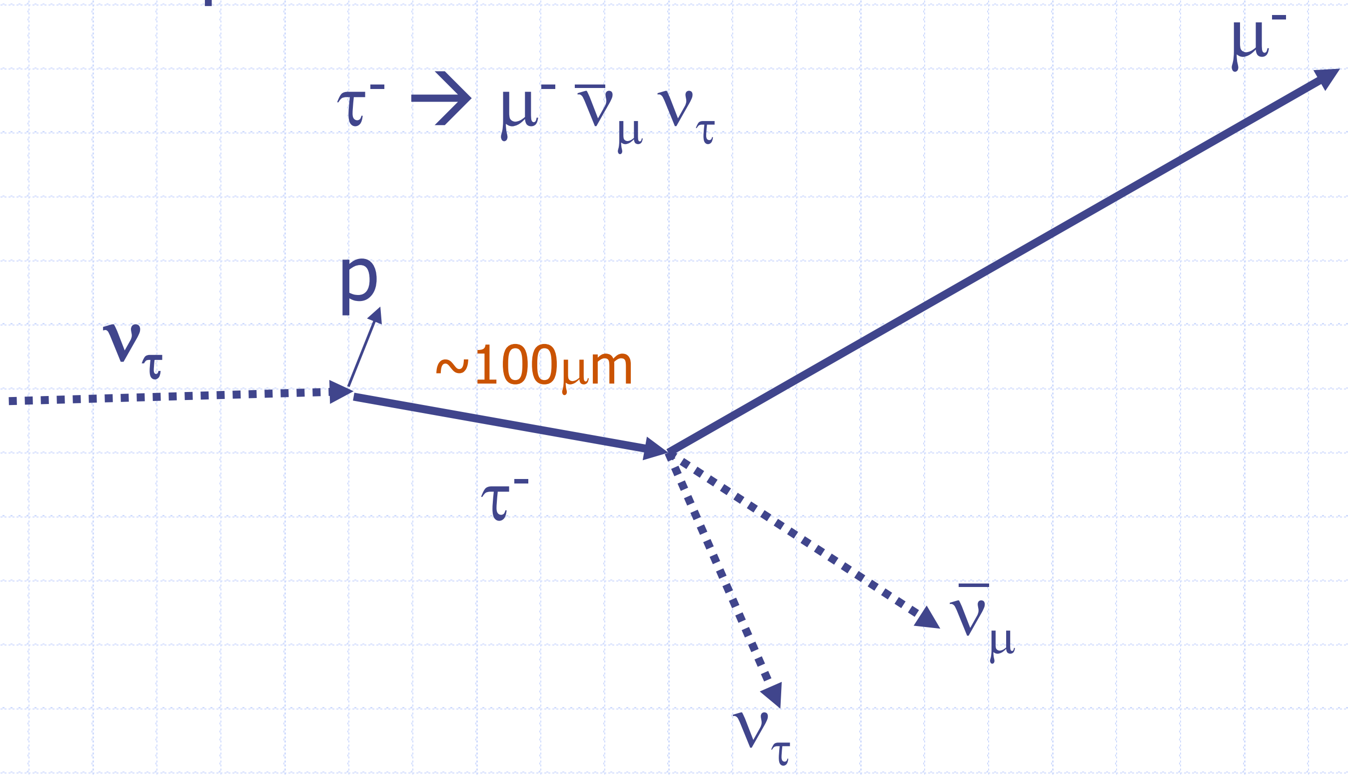

Detection of τ neutrinos 2

- Detect and identifiy mion
- Extrapolate back
- Check for a 'kink' in the sensitive volume – e.g. a thick photographic emulsion

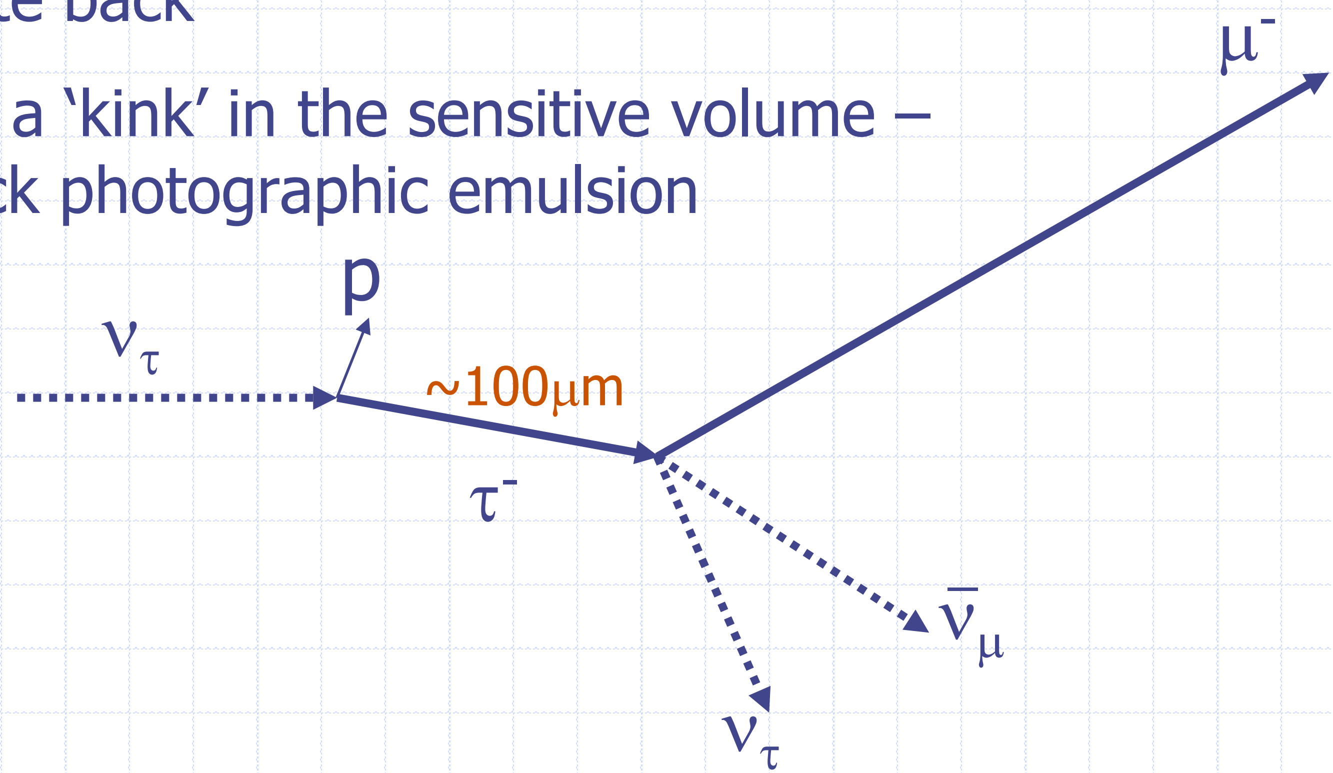

Detection of τ neutrinos 3

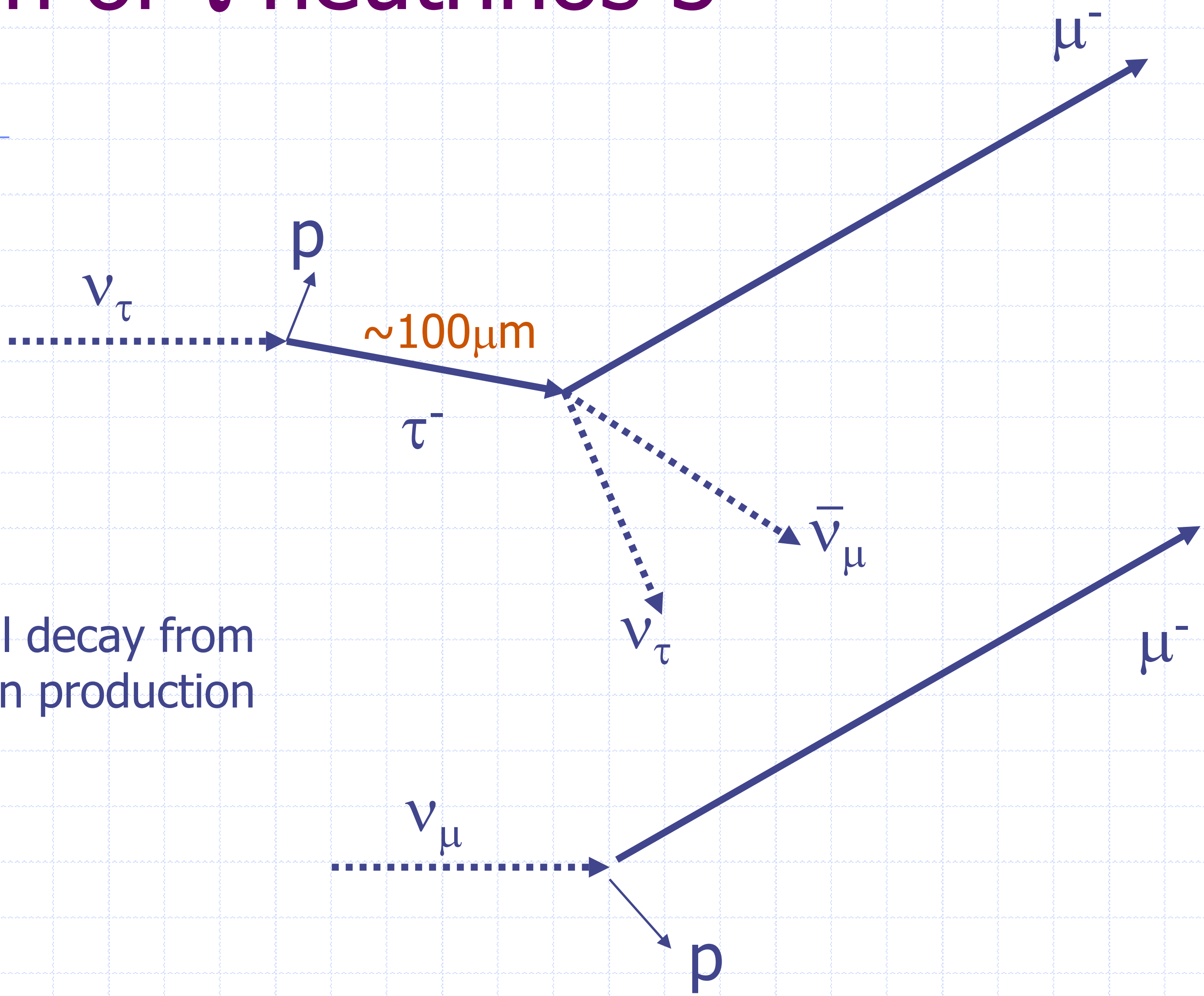

Separate signal decay from the direct muon production

Detection of τ neutrinos: OPERA

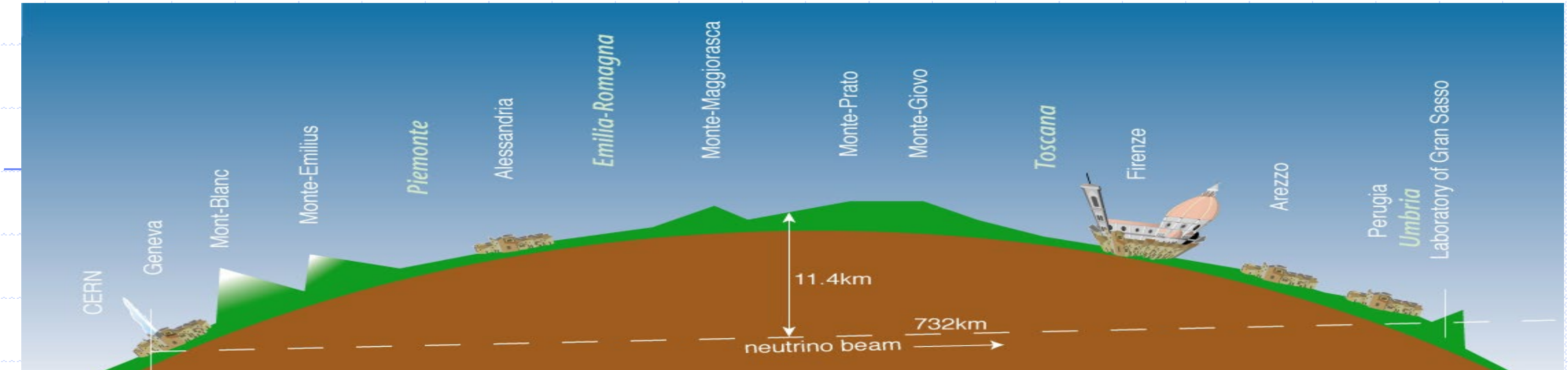

ν

8.3 kg $10X_0$

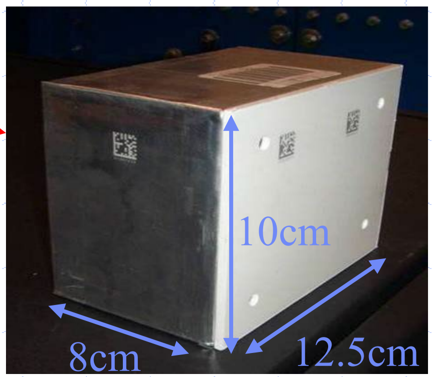

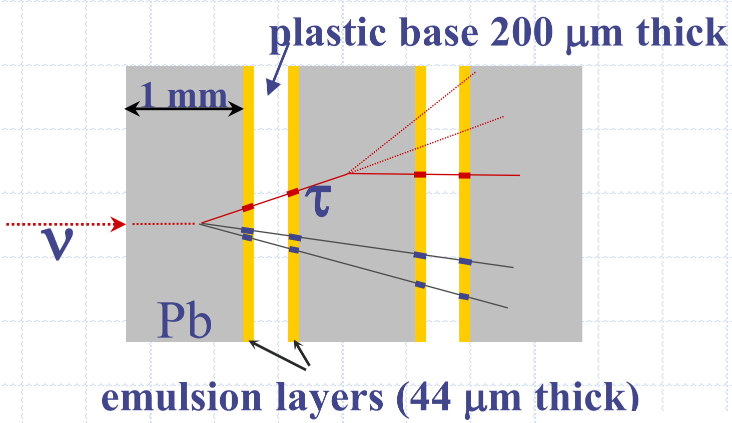

Detection unit: a brick with 56 Pb sheets (1mm) + 57 emulsion films

155000 bricks, detector total mass = 1.35 kton

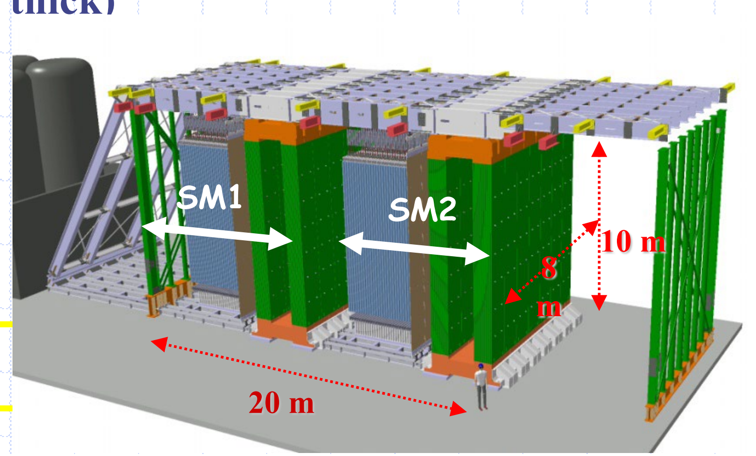

Detection of very high energy neutrinos (from galactic sources)

The expected fluxes are very low:

Need really huge volumes of detector medium!

What is huge? From $(100\text{m})^3$ to $(1\text{km})^3$

Also needed: directional information.

Again use: $\nu_\mu + n \rightarrow p + \mu^-$; μ direction coincides with the direction of the high energy neutrino.

AMANDA: use the Antarctic ice instead of water

Normal ice is not transparent due to Rayleigh scattering on inhomogenuities (air bubbles)

At high pressures (large depth) there is a phase transition, bubbles get partly filled with water-> transparent!

Originally assumed: below 800m OK; turned out to be much deeper.

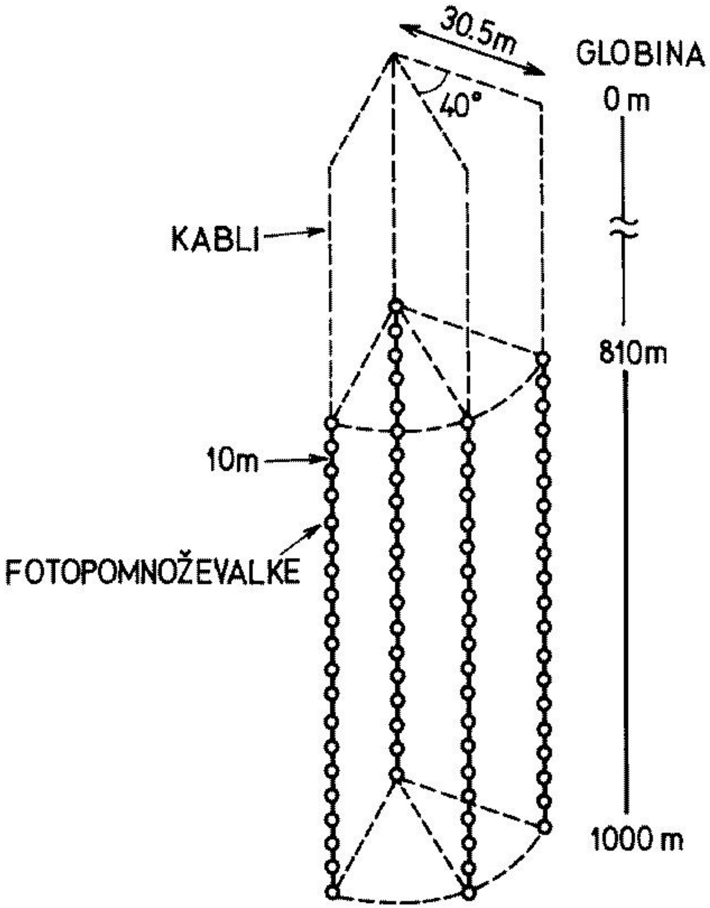

AMANDA

1993 First strings AMANDA A
1998 AMANDA B10 ~ 300 Optical Modules
2000 AMANDA II ~ 700 Optical Modules
2010 ICECUBE 4800 Optical Modules

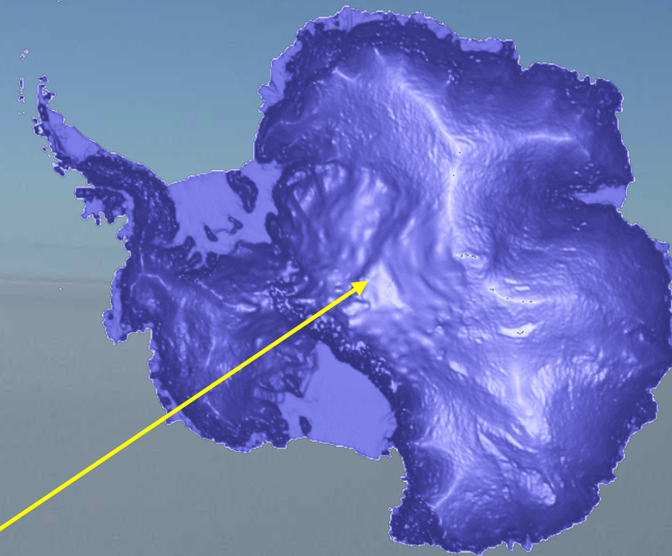

Amundsen-Scott South Pole station

Reconstruction of direction and energy of incident high energy muon netrino

For each event:

Measure time of arrival on each of the tubes

Cherenkov angle is known: $\cos\theta = 1/n$

Reconstruct muon track

Track direction -> neutrino direction

Track length -> neutrino energy

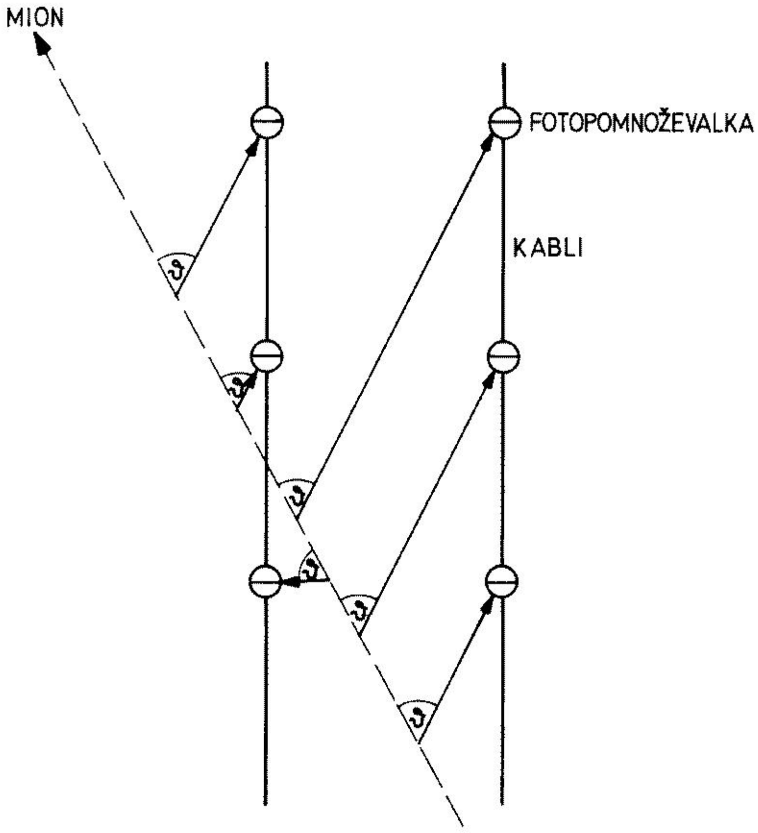

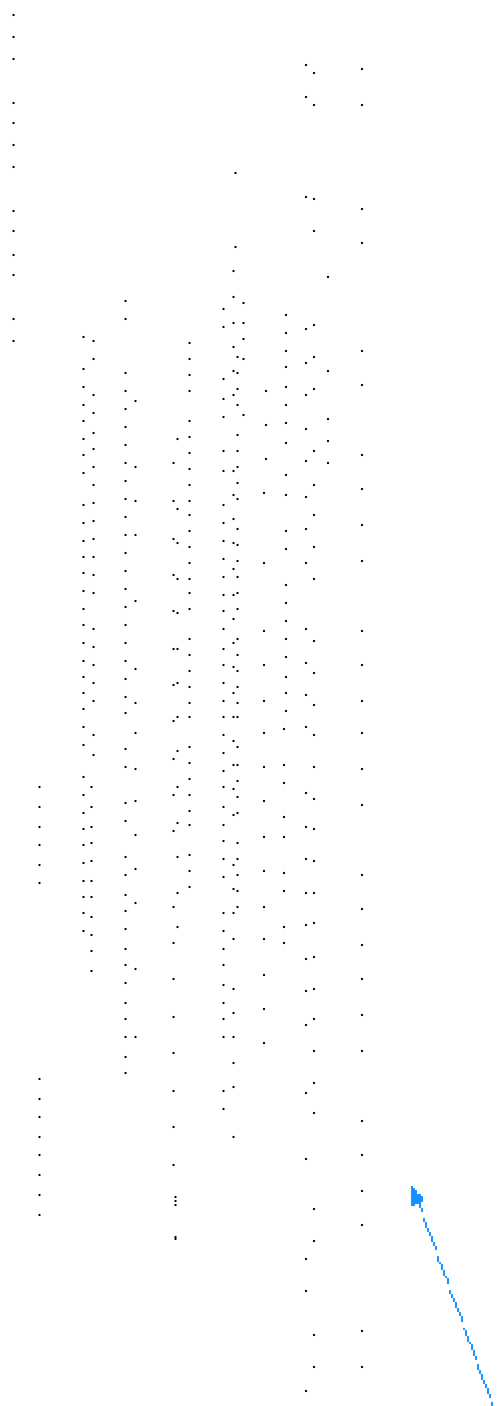

AMANDA

- Example of a detected event, a muon entering the PMT array from below

Neutrino detection arrays in water

Similar geometry can be used in a water based detector deep below the sea surface (say around 4000m)

- ANTARES (Marseille)
- Nestor (Pylos, SW Pelophonysos)
- Lake Baikal
- DUMAND (Hawaii) - stoped

Problems: bioluminescence, currents, waves (during repair works)

Lake Baikal: deployment, repair works: in winter, from the ice cover

NEUTRINO TELESCOPE NT-200

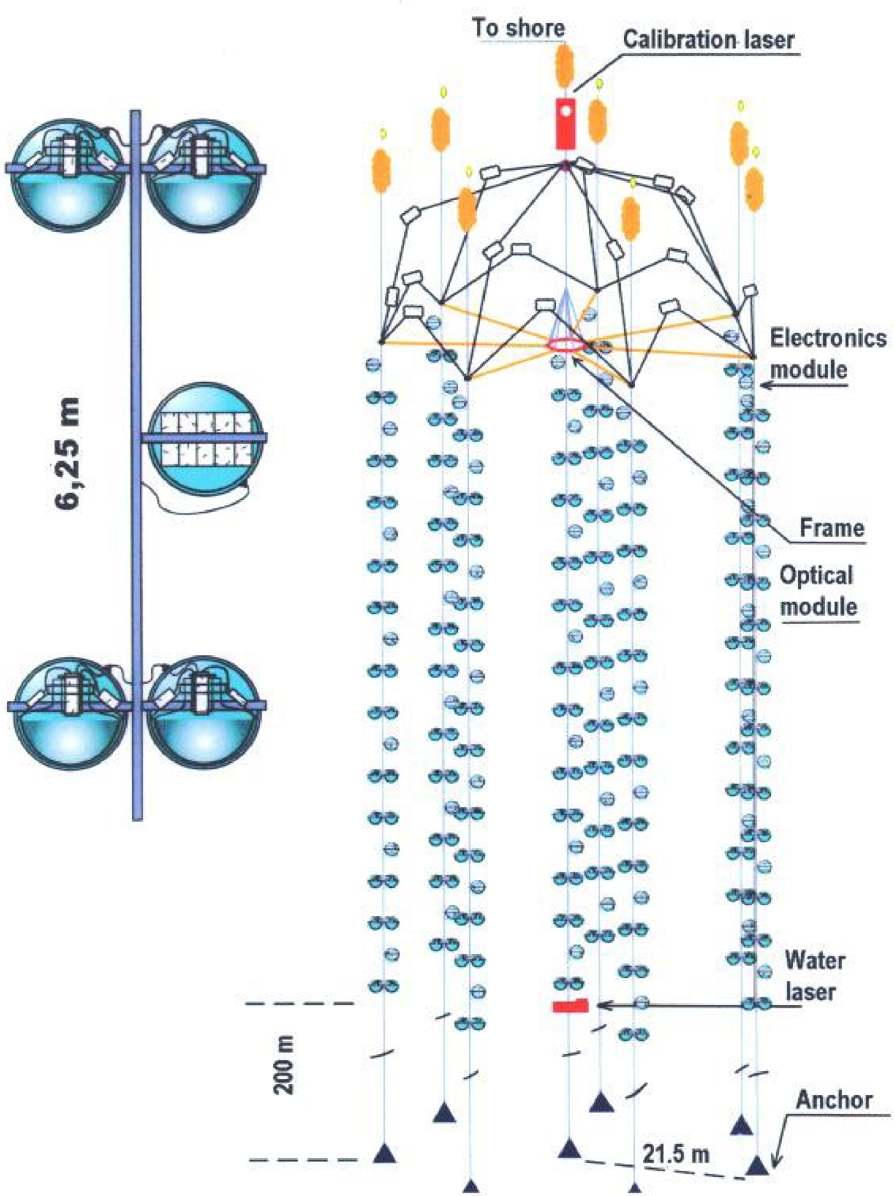

ron and
tion

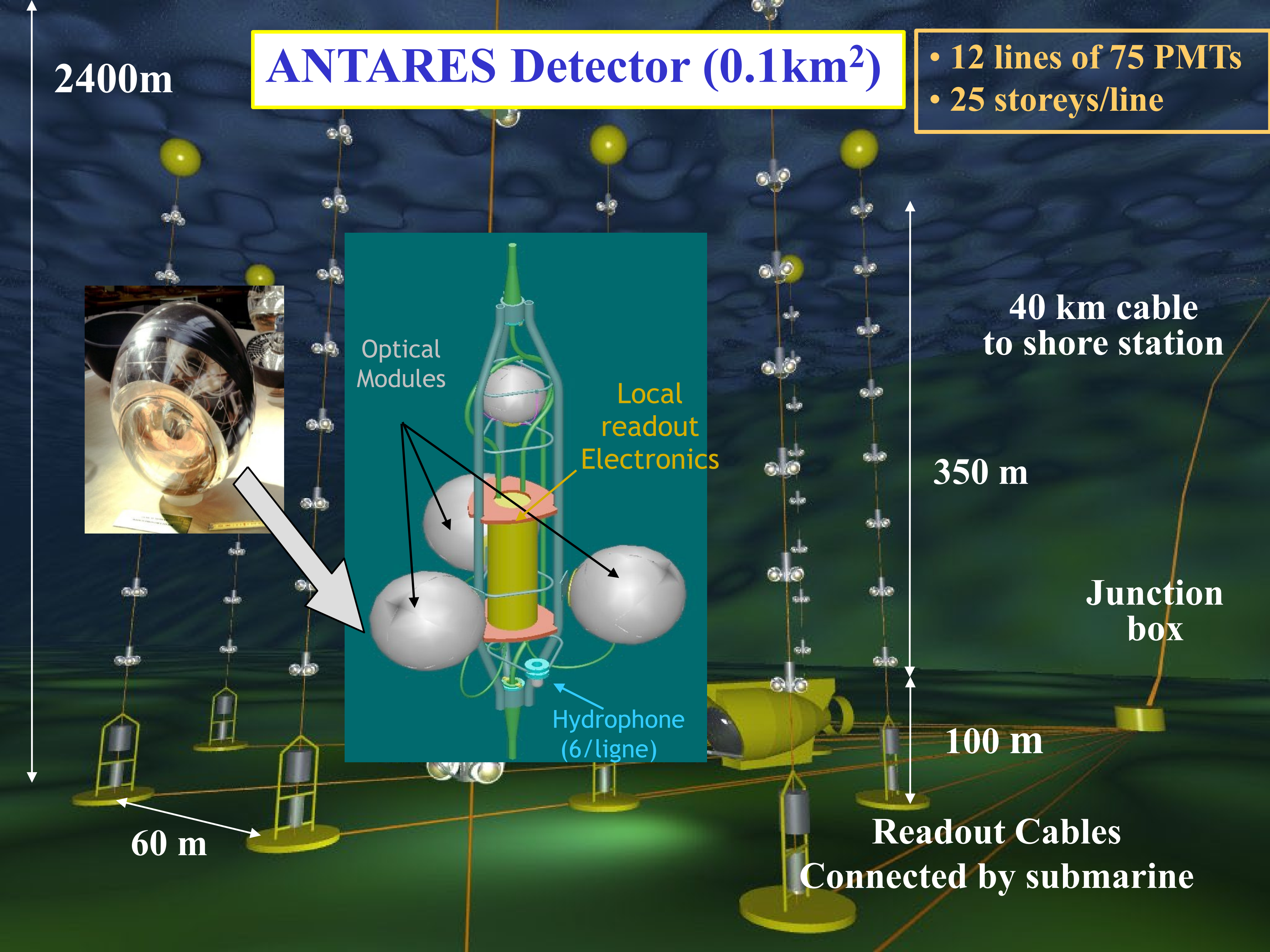
ANTARES Detector (0.1km^2)
• 12 lines of 75 PMTs
• 25 storeys/line
2400m
40 km cable
to shore station
Optical
Modules
Local
readout
Electronics
350 m
Junction
box
Hydrophone
(6/ligne)
100 m
60 m
Readout Cables
Connected by submarine

Generic Optical Module Components (from ANTARES)

LED Pulser

Optical coupling & (almost) index-matching gel

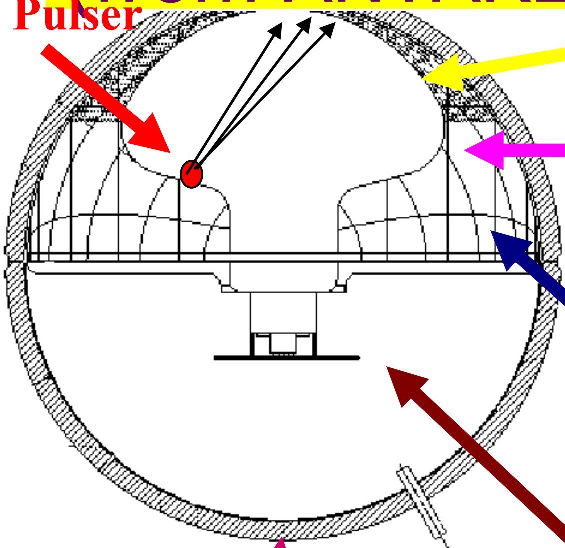

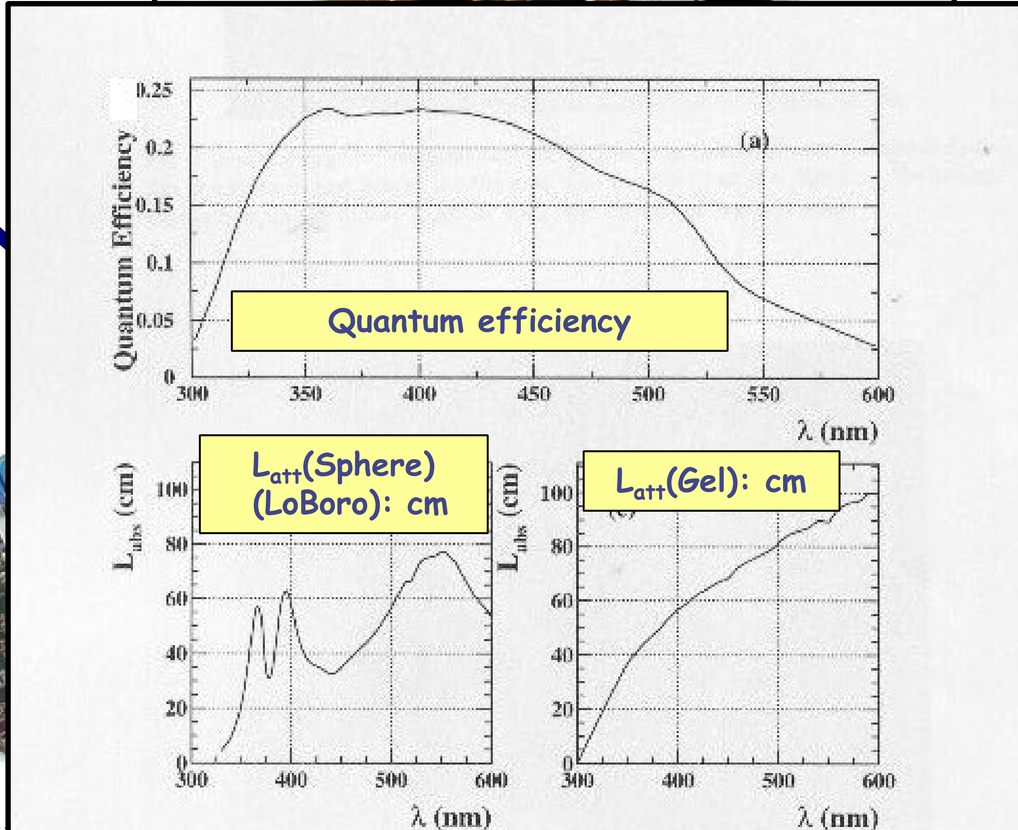

Glass Pressure Sphere

Activ

(Cock

Efficiency:(quantum ⊕ collection)>16%;

Region of sky observable by Neutrino Telescopes

AMANDA (South Pole)

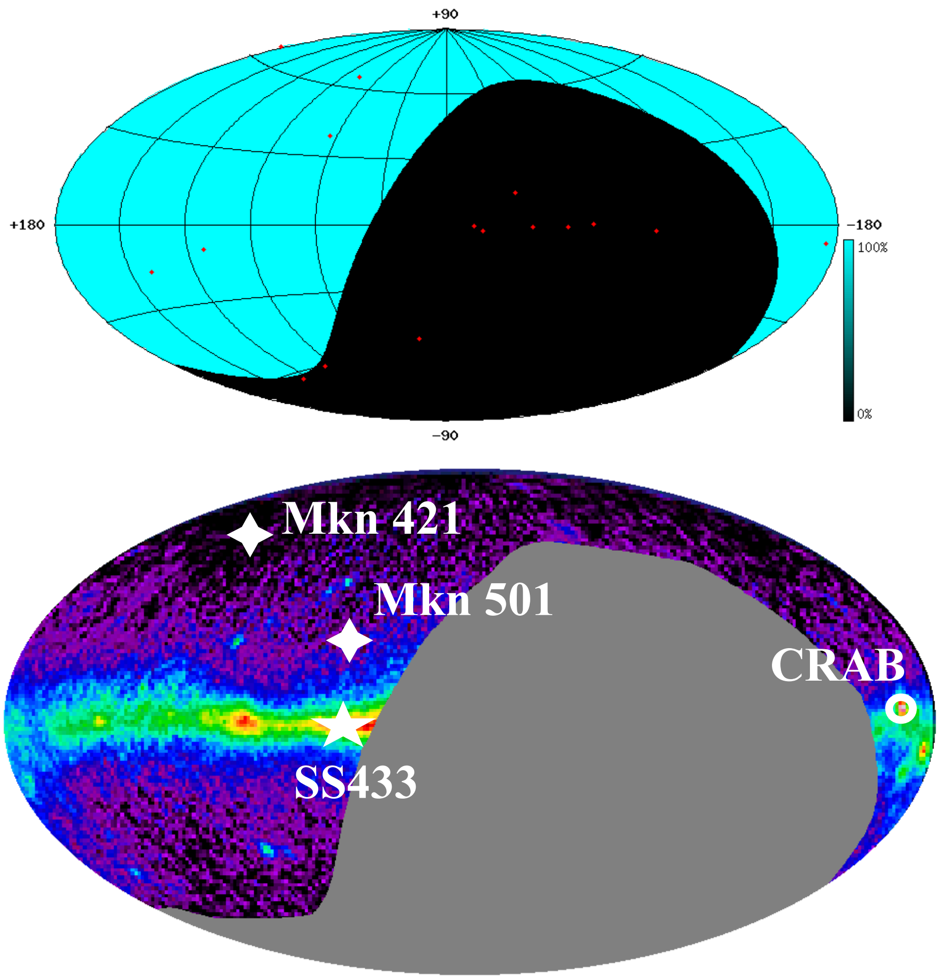

ANTARES (43° North)

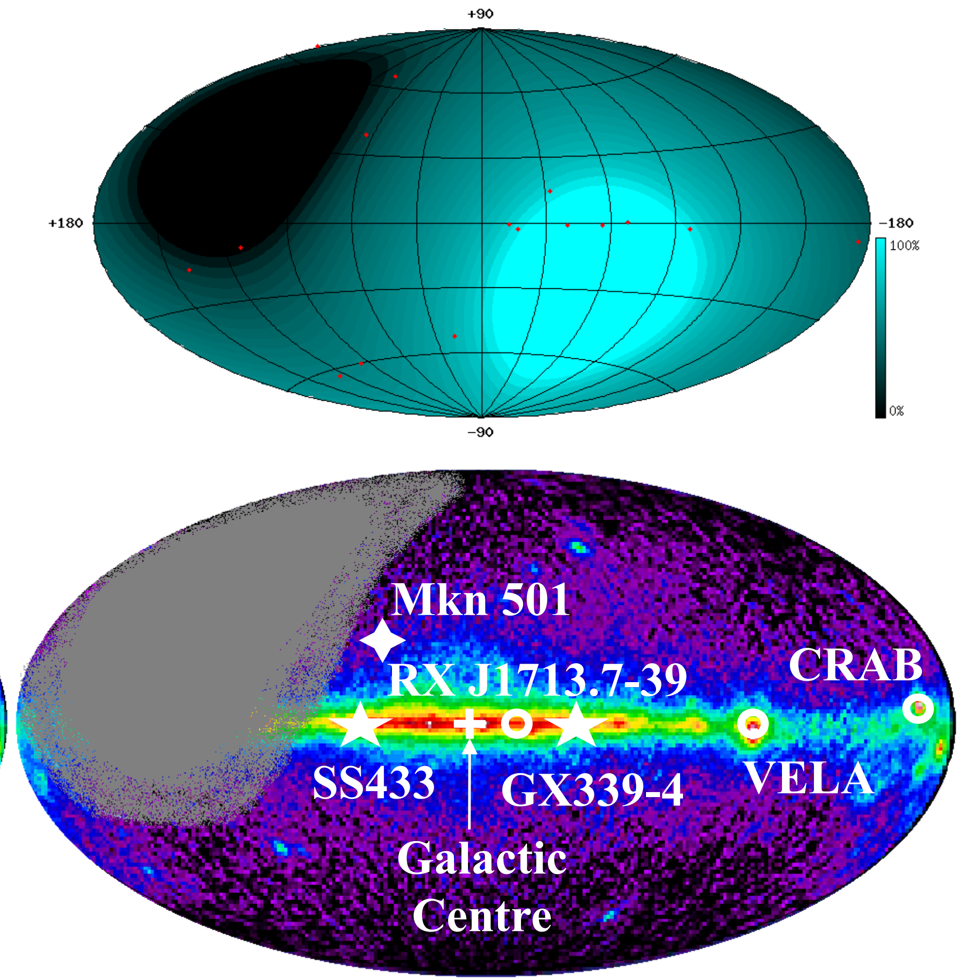

Next generation neutrino telescopes

Go for 1 km^3 detector volume!

- Ice cube
- KM3

AmandaII

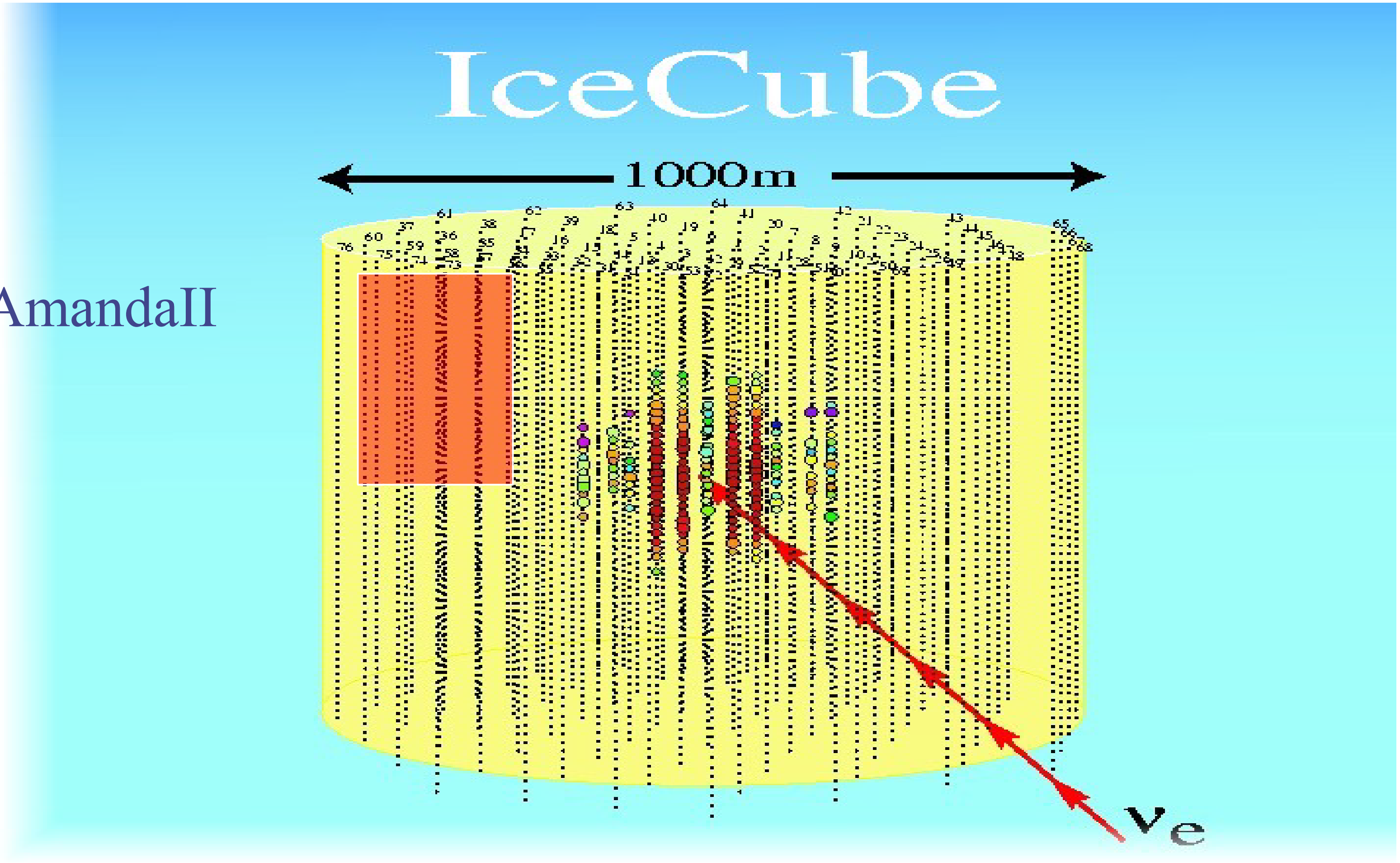

KM3NeT: EU FP6 Design Study

Participants: 8 countries, 34 institutes (ANTARES+NESTOR+NEMO+...)

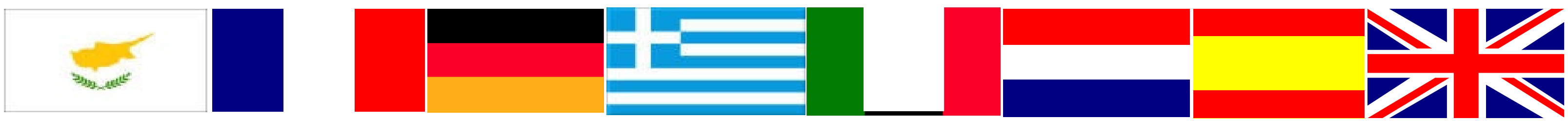

WORK PACKAGES

Astroparticle Physics	Physics Analysis	System and Product Engineering
Information Technology	Shore and deep-sea structure	Sea surface infrastructure
Risk Assessment Quality Assurance	Resource Exploration	Associated Science

KM3NeT: Site Choice?

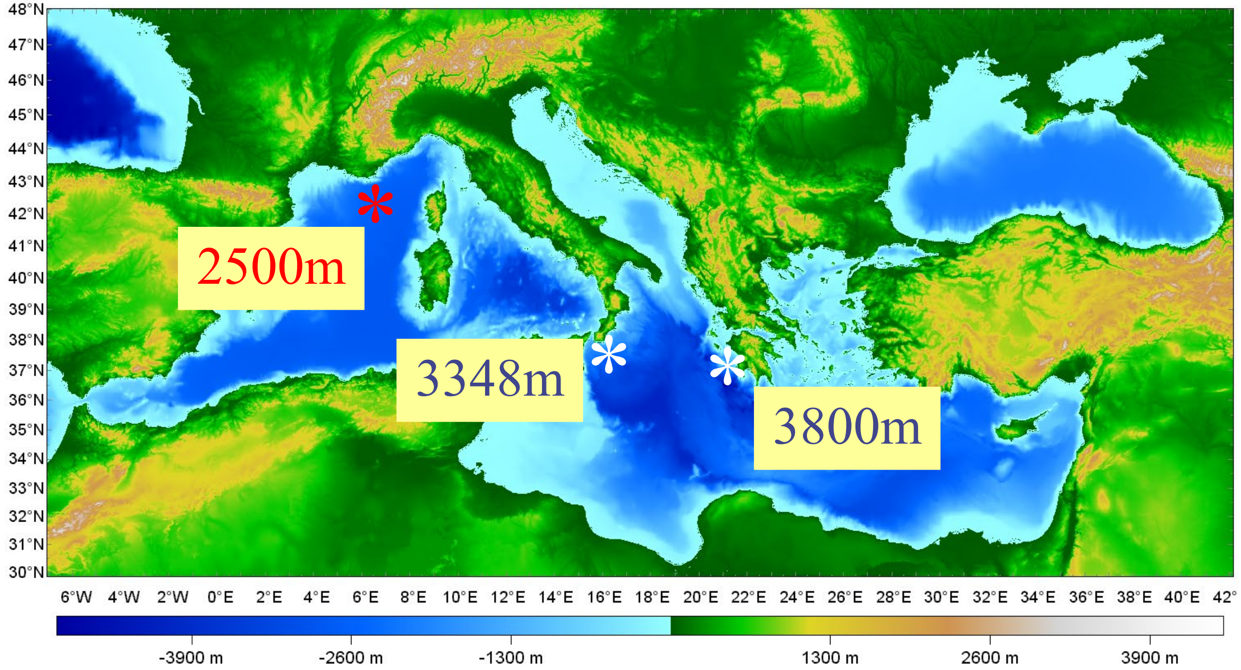

Additional slides

Detection of low energy neutrinos (from sun)

Solution to solar neutrino problem;
 Why is the ν_e flux at the earth's surface (e.g. Homestake) ~ 1/3 that expected from models of solar ν_e production?

Do ν's oscillate:

change flavour ➔ ν_e
➔ ν_μ
➔ ν_τ

Sudbury Neutrino Observatory, Ontario, Canada

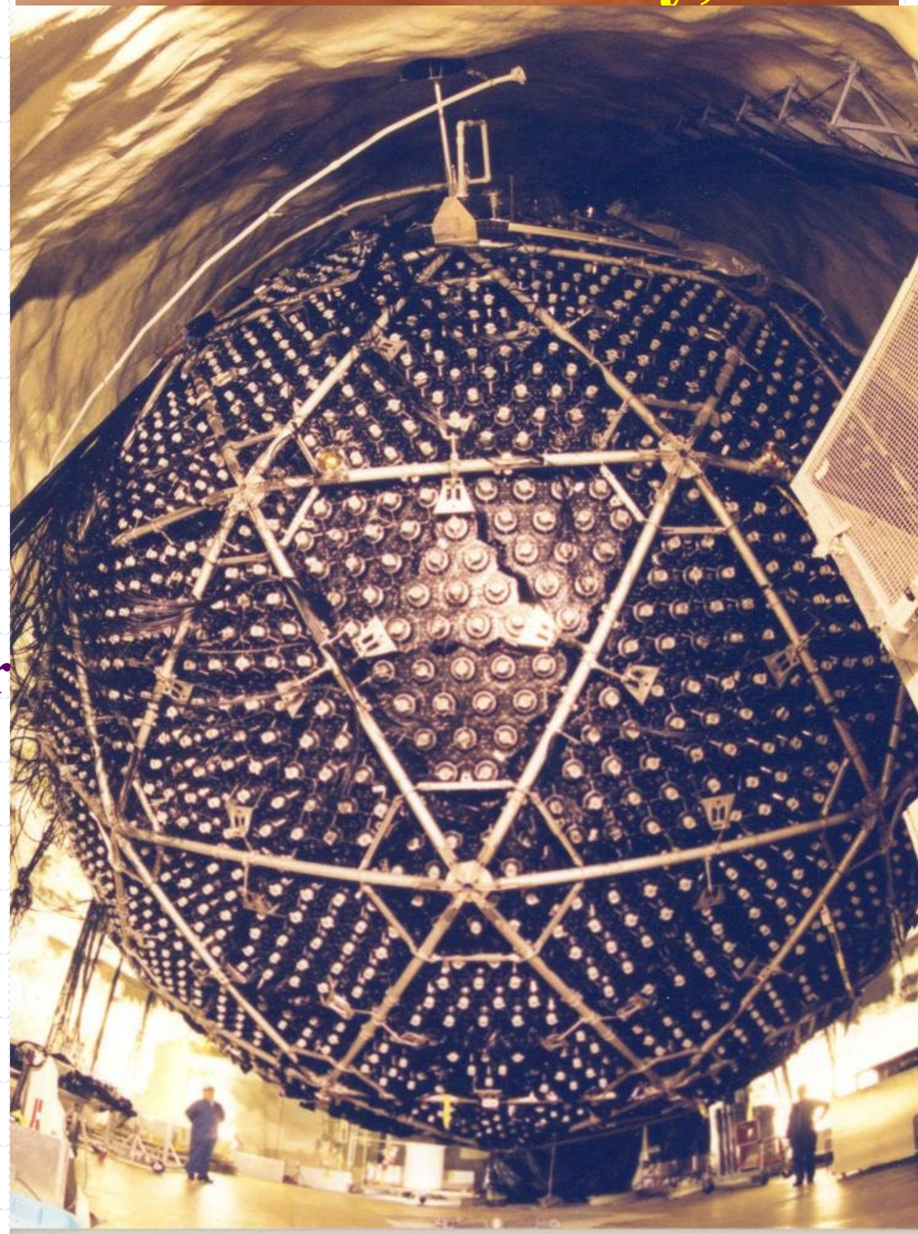

Pure Water
Radiation shield
in cavern Ø 22m,
Height 34m

1000 tonnes
Pure heavy water
in Ø=12m sphere

9456 8” PMTs
(Hamamatsu
R1408:
bi-alkali
photocathode)

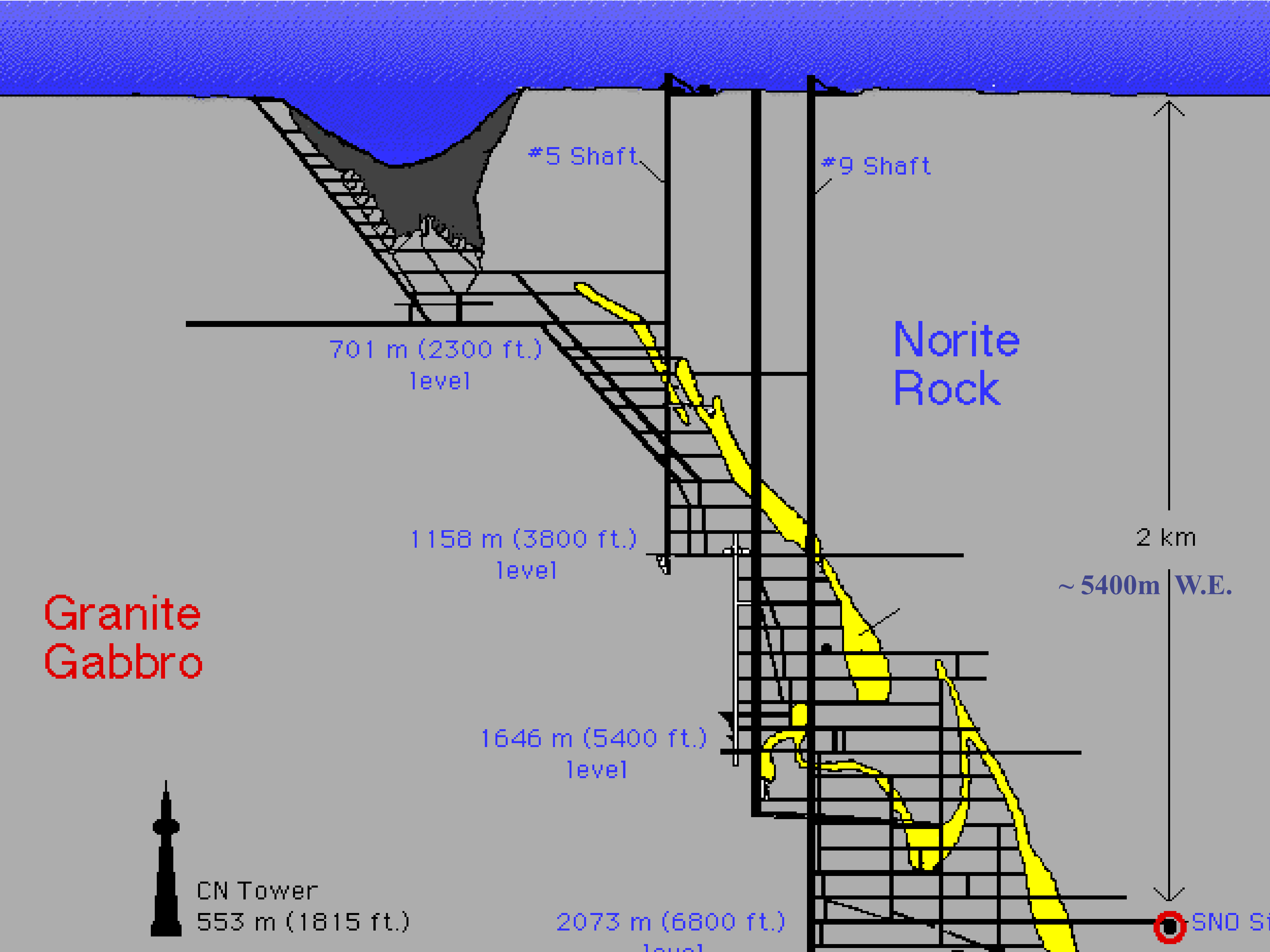

#5 Shaft
#9 Shaft
Norite Rock
701 m (2300 ft.) level
1158 m (3800 ft.) level
2 km
~ 5400m W.E.
Granite Gabbro
1646 m (5400 ft.) level
CN Tower
553 m (1815 ft.)
2073 m (6800 ft.)

Sudbury Neutrino Observatory

Due to presence of D_2O, SNO detector sensitive to all 3 neutrino flavours:

ν Reactions in SNO

CC $\nu_e + d \Rightarrow p + p + e^-$ → Č light

- Good measurement of ν_e energy spectrum
- Weak directional sensitivity $\propto 1 - 1/3\cos(\theta)$
- ν_e only.

NC $\nu_x + d \Rightarrow p + n + \nu_x$

- Equal cross section for all ν types

n captured by another deuteron ➔ γ scatters e ➔ Č light

ES $\nu_x + e^- \Rightarrow \nu_x + e^-$ → Č light